Economic Geology, v. 115, no. 7, pp. 1385–1412

The Onto Cu-Au Discovery, Eastern Sumbawa, Indonesia: A Large, Middle Pleistocene Lithocap-Hosted High-Sulfidation Covellite-Pyrite Porphyry Deposit

David R. Burrows,[1,†] Michael Rennison,[2] David Burt,[2] and Rod Davies[2]

[1] *Vale Global Exploration, Highway 17 West, Copper Cliff, Ontario, Canada P0M 1N0*

[2] *Cobre Nuevo Exploration Pty Ltd, 6 Moorak Street, Taringa, Queensland 4068, Australia*

Abstract

In 2013, a diamond drill program tested an extensive advanced argillic alteration lithocap within the Hu'u project on eastern Sumbawa Island, Indonesia. A very large and blind copper-gold deposit (Onto) was discovered, in which copper occurs largely as disseminated covellite with pyrite, and as pyrite-covellite veinlets in a tabular block measuring at least 1.5 × 1 km, with a vertical thickness of ≥1 km.

Copper and gold are spatially related with a series of coalesced porphyry stocks that intrude a polymictic diatreme breccia capped by a sequence of intramaar laminated siltstones, volcaniclastic and pyroclastic rocks, and overlain by andesite flows and domes. The porphyry intrusions were emplaced at shallow depth (≤1.3 km), with A-B–type quartz veinlet stockworks developed over a vertical interval of 300 to 400 m between ~100 and 500 m below sea level (bsl), 600 to 1,000 m below the present surface, which is at 400 to 600 m above sea level.

In the area drilled at Onto, the diatreme breccia, all porphyry intrusions and, to a lesser extent, the surrounding older andesite sequence have all been overprinted by intense subhorizontal advanced argillic alteration, zoned downward from illite-smectite, quartz-dickite to quartz-alunite and quartz-pyrophyllite ± diaspore alteration. The alteration package includes two particularly well-developed zones of residual quartz with vuggy texture in subhorizontal zones at shallow depth, the upper one is still porous but the lower horizon, ~100 m thick, is largely silicified and is located at or near the top of the quartz-alunite alteration.

Mineralization starts below the lowermost silicic horizon with more than 90% of the current resource in quartz-pyrophyllite-alunite and quartz-alunite alteration. Mineralization is dominated by a high-sulfidation assemblage of covellite-pyrite ± native sulfur largely in open-space fillings and replacements, but also as discrete pyrite-covellite and covellite only veins down to at least 1 km. Although the greatest amount of copper occurs as paragenetically late covellite deposited during formation of the advanced argillic alteration, approximately 60% of resource at 0.3% Cu cutoff still occurs within the porphyry stocks, indicating the porphyry stocks are a fundamental control on mineralization. There is considerable remobilization and dispersion of copper and, to a lesser extent, gold into the surrounding pre-mineral breccia and the late intermineral intrusions from the two earliest porphyry phases, resulting in quite consistent copper and gold grades throughout the currently delineated mineral resource. The very high sulfidation state of the mineralization is thought to be a consequence of the metal-bearing ore fluids cooling in the advanced argillic-altered host rocks in the absence of a rock buffer.

Early chalcopyrite-bornite ± pyrite mineralization with potassic ± chloritic and sericitic alteration is only preserved on the margins of the system and more rarely at depth in a few holes 600 m bsl (~1,100 m below surface) but makes up only a small proportion (~8%) of the current resource.

The Onto system is exceptionally young and formed rapidly in the middle Pleistocene and is not significantly eroded. A U-Pb zircon age for the andesite that caps the volcanosedimentary host rocks provides a maximum age of 0.838 ± 0.039 Ma, with a slightly younger porphyry zircon crystallization age of 0.688 ± 0.053 Ma. Re-Os dating of molybdenite that is associated with both the quartz vein stockwork and high-sulfidation assemblage copper mineralization shows overlap between 0.44 ± 0.02 and 0.35 ± 0.0011 Ma. $^{40}Ar/^{39}Ar$ ages for alunite within the advanced argillic alteration block ranges from 0.98 ± 0.22 to 0.284 ± 0.080 Ma, and alunite closely associated with covellite spans a period from 0.537 ± 0.064 to 0.038 ± 0.018 Ma.

Introduction

The upper parts of porphyry copper systems, mainly at shallower levels than their porphyry intrusions, are characterized by lithocaps comprising lithologically controlled zones of pervasive advanced argillic alteration with subvertical root zones that are structurally controlled (Sillitoe, 2010). Alteration is typified by advanced argillic alteration (Meyer and Hemley, 1967; Hemley et al., 1980) comprising quartz-dickite-kaolinite, quartz-alunite, and quartz-pyrophyllite ± diaspore as well as vuggy residual quartz and intensely silicified rocks. The term advanced argillic alteration is used in this sense for the above alteration types throughout the remainder of this manuscript.

High-sulfidation epithermal-style pyrite-gold-enargite ± covellite mineralization in these lithocaps has long been recognized to form at some distance above or adjacent to porphyry copper deposits (e.g., Sillitoe, 1983, 1999; Stoffregen, 1987), and a genetic relationship between porphyry and high-sulfidation epithermal deposits was proposed (Arribas et al., 1995; Hedenquist et al., 1998). High-sulfidation gold mineralization, particularly where subsequent supergene leaching has oxidized refractory sulfides, forms large, economically viable epithermal deposits such as Yanacocha, Pierina, and Al Lagunas Norte in Peru (Rainbow et al., 2005; Teal and Benavides, 2010; Cerpa et al., 2013) and Pascua Lama in Chile and Argentina (Chouinard et al., 2005). A few deposits have been exploited for both copper and gold, such as Lepanto in the Philippines, the Zijinshan deposit in China, and Bor in Serbia

† Corresponding author: e-mail, david.burrows@vale.com

ISSN 0361-0128; doi:10.5382/econgeo.4766; 28 p.
Digital appendices are available in the online Supplements section.

Submitted: September 18, 2019 / Accepted: April 13, 2020

(Hedenquist et al., 1998; Herrington et al., 1998; Pittuck, 2014; Chen et al., 2019), although these sulfide orebodies are generally small, ≤50 Mt with 1 to 2% Cu and a few g/t Au; an exception was El Indio, Chile, with locally bonanza gold grades (Jannas et al., 1990; Sillitoe, 1999).

This paper presents data on a very large copper-gold high-sulfidation epithermal/porphyry deposit recently discovered at Onto within the Hu'u project in Eastern Sumbawa, Indonesia, in which disseminated and vein mineralization occurs uniformly within a zone measuring ~1.5 × 1 km that is ≥1 km thick. Mineralization is predominantly hosted by multiple porphyry stocks that intruded to shallow levels in a diatreme vent complex. Copper is contained almost exclusively as covellite associated with pyrite, and there is a remarkable spatial and temporal relationship of high-sulfidation epithermal-style mineralization and mineralized porphyry stocks. The Onto deposit is remarkable in that more than 90% of the current resource occurs in quartz-pyrophyllite-alunite and quartz-alunite alteration that totally envelops the porphyry stocks and surrounding diatreme breccia down to depths >1 km. These relationships have implications for previously described porphyry-epithermal transition models (e.g., Muntean and Einaudi, 2001; Gustafson et al., 2004) and the spatial relationship between porphyry-style mineralization and high-sulfidation epithermal deposits (Arribas et al., 1995; Hedenquist and Taran, 2013). The relationships observed at Onto may also help determine whether advanced argillic alteration in lithocaps overprints porphyry-style mineralization or whether quartz-pyrophyllite-alunite alteration is an upward transition from quartz-sericite alteration forming from deeper ore fluids (e.g., Watanabe and Hedenquist, 2001). Finally, the Onto deposit is exceptionally young and formed rapidly in the last 500,000 years. This places some time constraints on the temporal relationships between cogenetic porphyry and high-sulfidation epithermal deposits, and the timing of advanced argillic alteration relative to high-sulfidation–style mineralization.

Exploration History

The Onto deposit is located in the eastern portion of Sumbawa Island in West Nusa Tenggara province, Indonesia, within the Hu'u 7th generation Contract of Work that covers 19,260 hectares (Figs. 1, 2). It is held by PT Sumbawa Timur Mining, a company owned 80% by Eastern Star Resources (a Vale subsidiary) and 20% by PT Antam Tbk.

Between 1995 and 1997, Aberfoyle (at that time the owner of Eastern Star Resources) conducted systematic exploration over the central parts of the Hu'u project area, mapping and collecting 4,697 surface samples and flying a 2,320-km fixed-wing aeromagnetic survey. The stream sediment and soil sampling carried out by Aberfoyle eliminated the possibility that an exposed porphyry system was present at Hu'u; however, some significant Mo soil geochemistry anomalies were located and a large lithocap area (9 × 5 km) of advanced argillic alteration was identified. Aberfoyle drilled 11 holes for a total of 5,528 m, testing geochemical anomalies (particularly soil Mo anomalies) and drilling under some of the silica ledges. The highlights of Aberfoyle's exploration included a trench with 100 m at 0.13% Cu and 0.23 g/t Au, and a best drill intersection of 106 m at 0.14% Cu and 0.08 g/t Au in andesite in drill hole HGD003 (Fig. 2). Following a corporate takeover, the new owner of Aberfoyle sold its interest in Eastern Star Resources to a private individual in 1999 and the CoW was subsequently placed into suspension in 2000 when a new investor could not be found.

Vale reviewed the Hu'u project in mid-2008 and was attracted by the potential for porphyry copper mineralization associated with and underlying the large lithocap with quartz-alunite-dickite-kaolinite alteration with widespread silicification identified by Aberfoyle. Vale negotiated an Option Agreement with the owners of Eastern Star Resources in 2009 and subsequently acquired Eastern Star Resources in 2012.

In February 2011, a discrete magnetic high in an aeromagnetic survey associated with a soil Cu-Au-Mo-Pb-As anomaly was drilled at the Humpa Leu East prospect (HLE, Fig. 2). The first hole at this prospect, VHD001, intersected 414 m at 0.45% Cu and 0.26 g/t Au, starting at 138 m downhole. Copper-gold ± molybdenum mineralization at Humpa Leu East is associated with an early diorite intrusion in biotite-magnetite alteration and associated A-B quartz veinlet stockwork. Subsequent drilling between April 2011 and April 2012 outlined a small copper-gold resource (0.5% Cu, 0.5 g/t Au). The resource is small because the pencil-shaped early diorite porphyry, measuring only ~150 (NW-SE) × 80 m (E-W) × 250 m vertical, was surrounded and stoped out by later intermineral and late porphyries, with lower copper grades.

Encouraged by the discovery of a moderate-grade albeit small porphyry at the Humpa Leu East, plus the large extent of the advanced argillic alteration (defined by kaolinite, dickite, alunite and, more rarely, pyrophyllite alteration and silicification), Vale continued to assess the lithocap by mapping, soil sampling, and a high-resolution helicopter-borne magnetic/radiometric survey flown along 100-m-spaced lines. A series of holes were drilled in 2012 to 2013, moving progressively to the southwest from Humpa Leu East (Fig. 2). Holes were typically drilled at steep angles to 800 m depth, on the premise that porphyry mineralization might be located at some depth beneath the outcropping lithocap.

One of the final holes in this step-out program was to test the Onto prospect area, which has a small magnetic high anomaly with subtle Cu anomalies in soils (six samples between 100 to 160 ppm Cu, without other metal anomalies). Crucially, mapping in the Onto prospect area had identified several mineralized clasts with covellite hosted by probable late-mineral phreatic breccias, and their recognition was a key observation that led to the decision to drill test the Onto prospect. Although not fully realized at the time, the subtle copper-only soil anomalies are related to these phreatic breccia dikes.

Drill hole VHD034, drilled in June 2013 (Figs. 2, 3), intersected 390 m of relatively unaltered magnetite-bearing andesite flows, underlain by a zone of quartz-dickite-kaolinite ± pyrophyllite alteration approximately 100 m thick, followed by a subhorizontal silicified vuggy residual quartz horizon approximately 80 m thick, composed almost entirely of quartz with only minor alunite ± dickite. Below this horizon, starting at 548 m drill depth, the hole intersected 287 m at 0.97% Cu and 1.13 g/t Au in vuggy-textured residual quartz and quartz-alunite alteration. Copper occurred almost entirely as covellite associated with pyrite and native sulfur, with minor enargite. The hole ended at 835 m (due to drilling capacity)

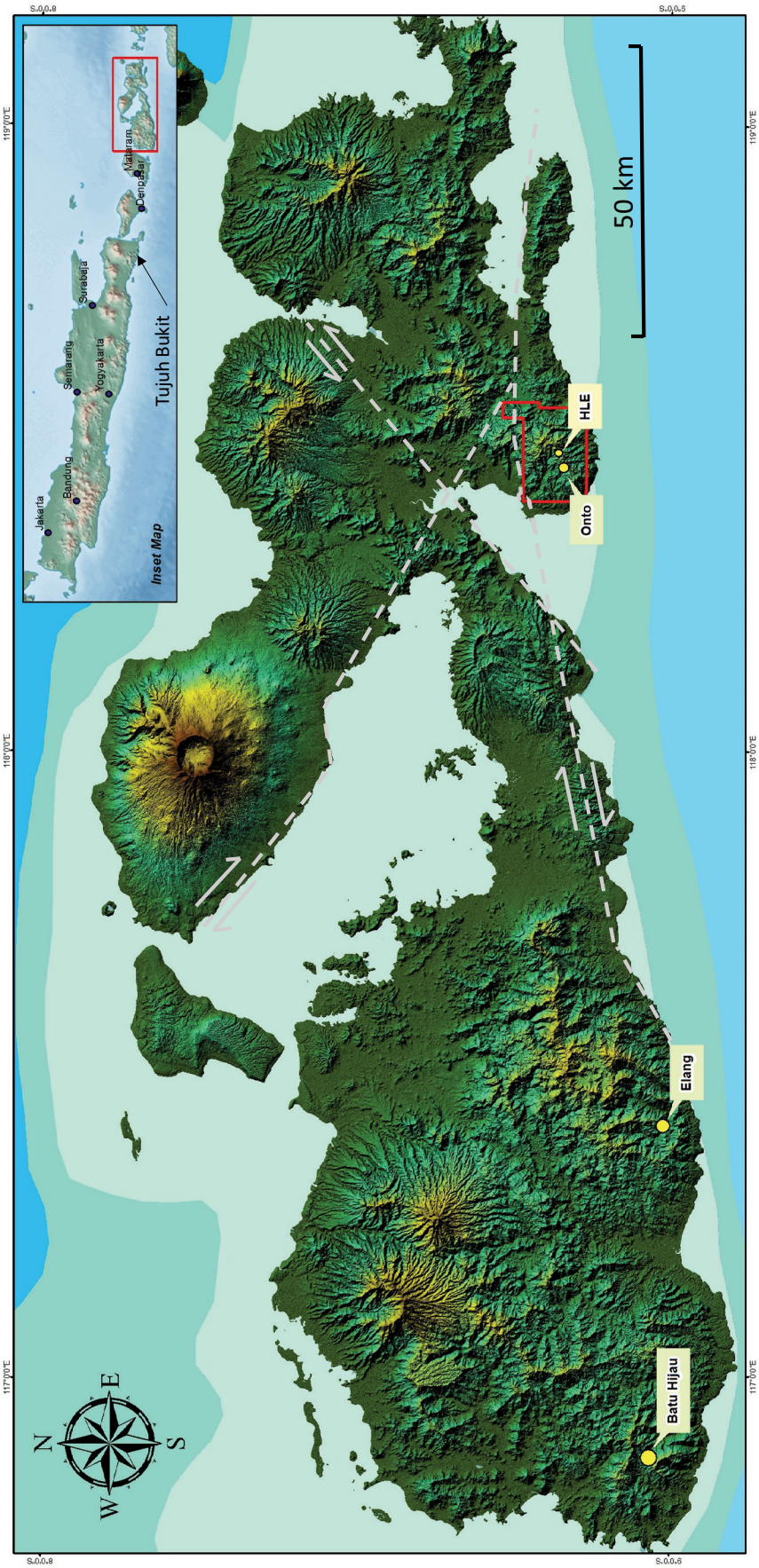

Fig 1. Satellite image of Sumbawa island showing the outline of Hu'u Contract of Work (CoW) in red, the relative positions of Humpa Leu East (HLE) and the Onto discovery area and prominent regional faults (see text). The location of the Batu Hijau and Elang porphyry deposits in western Sumbawa are shown as well as the location of the Tujuh Bukit-Tumpangpitu porphyry high-sulfidation Cu-Au deposit in Java (see inset).

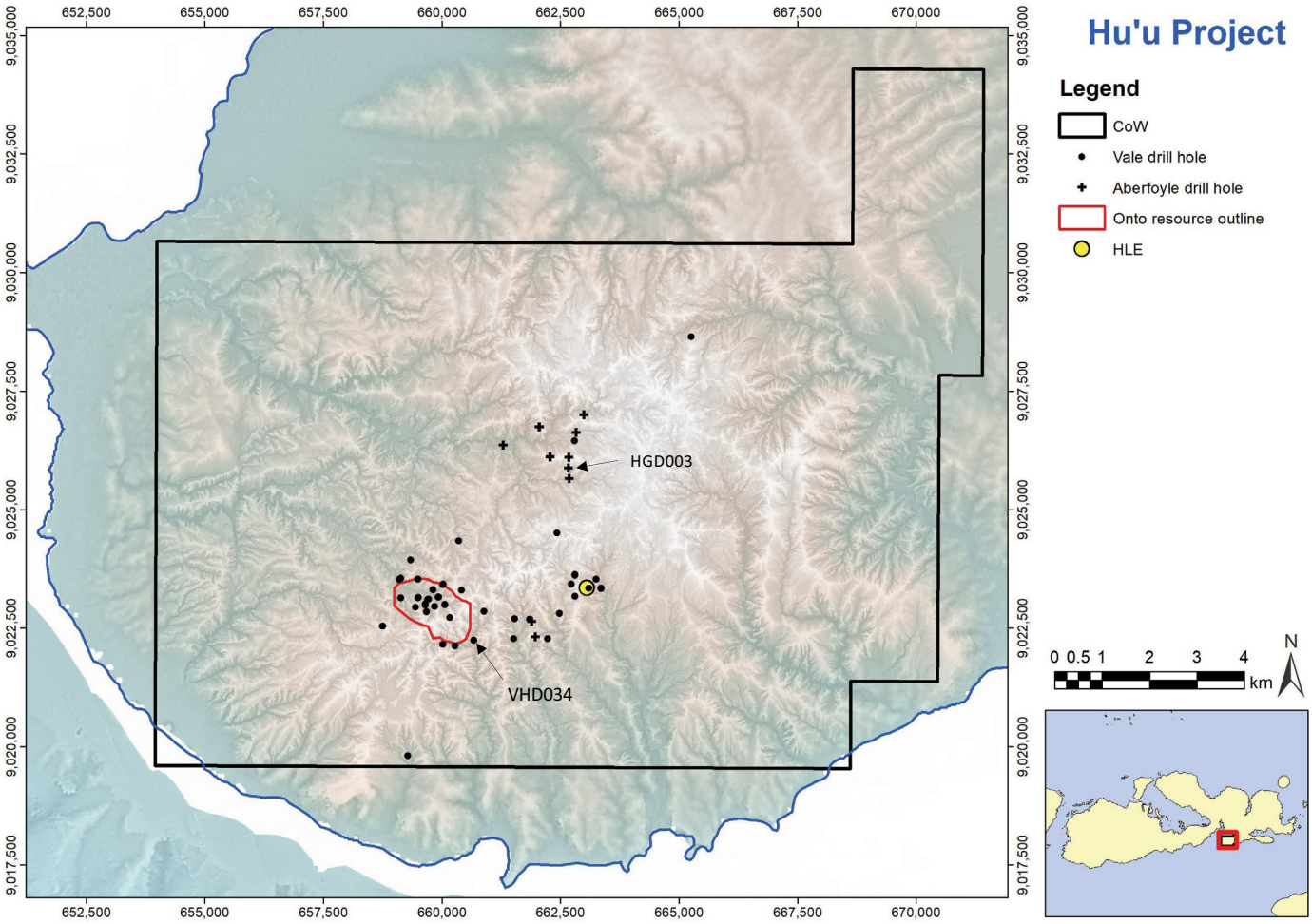

Fig. 2. Outline of the Hu'u Contract of Work property on topography showing location of Onto resource projected to surface (red outline) and the position of the HLE (Humpa Leu East) prospect (yellow dot). Drill holes are shown as small circles (Vale) and crosses (Aberfoyle). Note that in some cases multiple holes have been drilled from the same location but are only indicated by a single symbol. The Onto discovery hole (VHD034) and best Aberfoyle drill hole (HGD003) are also indicated.

in covellite-pyrite mineralization with 0.6% Cu and 2 g/t Au in an intense quartz vein stockwork (A-B style) within quartz-alunite and vuggy residual quartz alteration.

The next hole, VHD035, was drilled at –55° from a kilometer to the northwest back toward VHD034 and intersected a similar grade interval but without any quartz vein stockwork (Fig. 3). VHD036 drilled from the same site as VHD035 and at –55° to the south intersected lower-grade mineralization and passed out of advanced argillic alteration into muscovite-chlorite alteration. A nearly vertical hole from the same site, VHD037, was the first drill hole that revealed the full vertical extent of the mineralization as it terminated in mineralization at 1,485 m after intersecting 948 m at 1.26% Cu and 0.7 g/t Au. However, there was still a possibility that this hole had drilled down a narrow high-grade structure. Finally, in April and May 2014, VHD044 and VHD045 were drilled at –80° and –75° to the south and north, respectively, from a drill site 500 m northwest of VHD037, and both intersected similar grades to VHD037, indicating an impressive lateral extent of mineralization of at least 700 m in a NE-SW direction (Fig. 3; Table 1).

Up to the end of April 2019, a total of 64 drill holes (61,009 m) have been completed at Onto (Fig. 3). Twenty-six of these holes intersected wide intervals of mineralization at similar grades to the discovery hole over core lengths of up 1,140 m (Table 1). Several drill holes also intersected higher-grade mineralization in a zone above the main mineralized zone, over 10- to 30-m intervals (e.g., 24 m at 6.9% Cu and 0.42 g/t Au in VHD063 and 16 m at 12.1% Cu and 0.12 g/t Au in VHD072; Table 1). This zone is not currently included in the resource.

The Onto deposit currently has an indicated resource of 0.76 billion tonnes (Gt) at 0.93% Cu, 0.56 g/t Au, 5 g/t Ag, and 350 ppm As (7 Mt contained Cu, 13 Moz Au) and an inferred resource of 0.96 Gt at 0.87% Cu, 0.44 g/t Au, 3 g/t Ag and 350 ppm As (8.3 Mt contained Cu, 14 Moz Au). In addition to these resources, an exploration target of 0.6 to 1.7 Gt at 0.4 to 0.7% Cu and 0.2 to 0.3 g/t Au has been delineated in a surrounding envelope based on drilling at approximately 200 × 200- to 400 × 400-m centers (P.T. Sumbawa Timur Mining, 2020). The limits of this mineralized envelope are not closed in all directions and additional drilling is planned to determine the potential for economic extraction. The vast majority of these resources (>90%) occur as covellite-pyrite mineralization within quartz-alunite and quartz-pyrophyllite ± alunite and diaspore alteration zones.

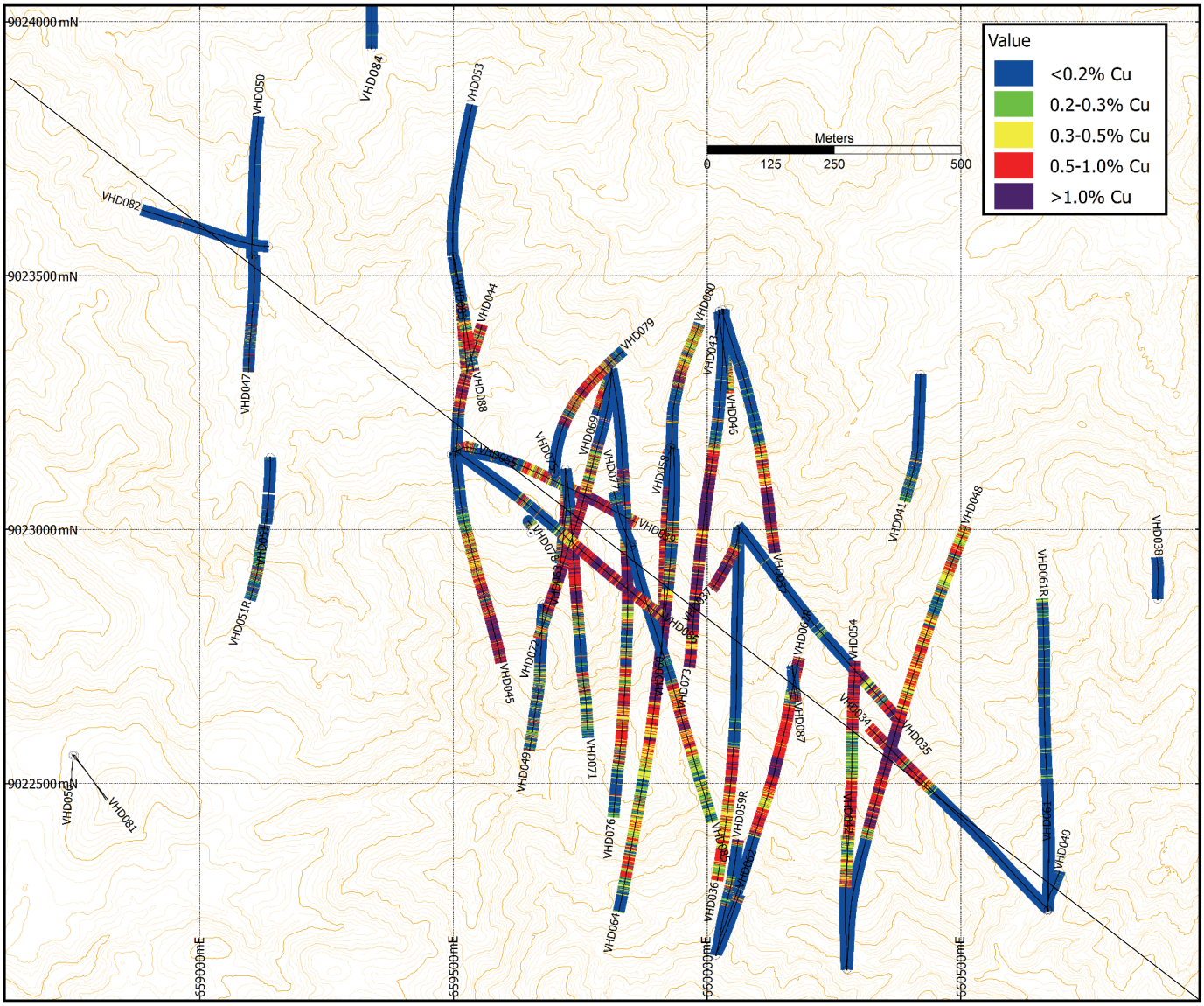

Fig. 3. Map of Onto drill hole distribution, projected to surface map showing elevation contours. Grid lines 500 m apart. Copper grades indicated by colors along drill hole traces; blue <0.1% Cu, green 0.1 to 0.3%, yellow 0.3 to 0.5%, orange 0.5 to 1% and red >1% Cu. The section line in Figs. 4a and b is from southeast corner (VHD040) to northwest corner (VHD050). Drill hole VHD052 (not shown) is 1 km directly north of VHD041. Black line indicates position of SE-NW longitudinal sections in Figures 4a, b and 8.

Regional Geology

The island of Sumbawa forms part of the productive Sunda-Banda volcanomagmatic arc and consists of an early Miocene to Holocene volcanic arc constructed on oceanic crust (Garwin et al., 2005). The Batu Hijau copper-gold mine and the large Elang project, both porphyry deposits (Garwin, 2002; Maryono et al., 2018), are located near the south coast in the western third of Sumbawa, approximately 175 and 120 km, respectively, west of the Hu'u Contract of Work. The recently discovered Tujuh Bukit (Tumpangpitu) porphyry and high-sulfidation epithermal deposit is located on the south coast of eastern Java (Fig. 1) also within the Sunda-Banda arc (Harrison et al., 2018).

Quaternary stratovolcanoes, including Tambora, form the northern part of Sumbawa and indicate a northward migration and progressive change from calc-alkaline to shoshonitic affinities with time from the older and more eroded southern margin of the island (Garwin, 2002). U-Pb age dating of 362 zircons collected from the heavy mineral concentrates in the six catchments draining the Hu'u project area (GEMOC, 2013) indicates a progressive development of andesitic volcanism with individual zircons recording magma chamber crystallization age ranges of 5.2 to 0.3 Ma and a principal age range of 2.7 to 0.3 Ma with sample peak ages of 1.1 to 0.7, 1.7 to 1.5, and 2.5 to 2.3 Ma. Even though the main locus of recent volcanic activity moved to the northern margin of Sumbawa, volcanism continued in the Hu'u area to at least ~500,000 years ago, given the very youngest zircon ages may be affected by Pb loss and have not been corrected for initial ^{230}Th disequilibrium.

Table 1. Showing Significant Intersections; (drill holes not shown were largely terminated early, or were drilled for other reasons—geotechnical, hydrogeology, more regional, etc.)

Drill hole	From (m)	To (m)	Interval length (m)	Cu grade (%)	Au grade (g/t)	As grade (ppm)
VHD034	548	835.2 (EOH)	287.2	0.97	1.13	503
VHD035	592	810.8 (EOH)	218.8	0.84	0.6	595
VHD036	698	1,113.4 (EOH)	415.4	0.59	0.26	182
VHD037	536	1,484.6 (EOH)	948.6	1.26	0.7	435
VHD039	430	450	20	1.48	0.43	192
	498	1,165.2 (EOH)	667.2	0.97	0.51	376
VHD042	534	582	48	2.26	2.5	570
VHD044	424	1,201.4 (EOH)	777.4	0.97	0.55	553
VHD045	640	1,,501.6 (EOH)	861.6	0.95	0.41	445
VHD046	932	1200.3 (EOH)	268.3	0.54	0.2	242
VHD048	522	1,523.4 (EOH)	1,001.4	0.75	0.57	219
VHD051R	972	1112	140	0.48	0.18	194
VHD054	492	1,500.1 (EOH)	1,008.1	0.66	0.47	263
VHD055	402	1168	766	0.99	0.5	677
VHD057	818	1,229.1 (EOH)	411.1	0.93	0.52	303
VHD058	322	376	54	1.66	0.08	784
	650	1,500.0 (EOH)	850	1.08	0.51	324
VHD060	312	1,451.7 (EOH)	1,139.7	1.02	0.55	312
VHD062R	622	1,499.4 (EOH)	877.4	0.77	0.69	163
VHD063	408	432	24	6.89	0.42	1834
	486	1,304	818	0.93	0.51	321
VHD064	316	408	92	0.52	0.07	399
	586	1,466	880	0.97	0.59	184
VHD067	326	530.0 (EOH)	204	0.67	0.27	898
VHD069	514	1,420	906	0.73	0.29	310
VHD071	350	966	616	0.81	0.43	375
	1,106	1,306	200	0.47	0.1	280
VHD072	358	374	16	12.1	0.12	2,153
	499.5	1,396.6 (EOH)	897.1	1.06	0.58	457
VHD073	730	1,471.3 (EOH)	741.3	1.29	0.9	274
VHD076	388	422.5	34.5	4.71	0.31	1243
	562	950	388	1.12	0.84	471
	992	1,382	390	0.57	0.2	229
VHD078	468	751.0 (EOH)	283	0.44	0.23	369
VHD079	534.5	658	123.5	2.18	1.04	851
	684	1,386	702	0.92	0.35	794
VHD080	752	1,502	750	0.8	0.3	486
VHD083R	584	928	344	0.71	0.48	308
	952	1,150 (EOH)	198	0.69	0.5	761
VHD085	644	1,220.0 (EOH)	576	0.63	0.24	105
VHD086	502	1,016.0 (EOH)	514	1.35	0.78	197
VHD087	648	830.3 (EOH)	182.3	0.9	0.67	223
VHD088	350	596	246	0.51	0.23	394

EOH = end of hole; these lengths are downhole intercepts; no attempt has been made to convert these to "true thickness"

The present topography in the Hu'u area appears to reflect an eroded portion of an original stratovolcano (Figs. 1, 2) and, based on a topographic reconstruction from the youngest lava dip slopes near Onto, the area may have reached an elevation of about 1,200 to 1,300 m above sea level (asl). The current elevation in the Onto area reaches 660 m with steeply incised river valleys. The area is jungle-covered and normal access is by helicopter.

A seismotectonic study (Pownall and Lister, 2015) indicates the Hu'u project area is at the intersection of several important fault zones. A major NW-trending sinistral fault is projected through Hu'u area from the southwestern side of Tambora volcano and a major sinistral fault is also indicated running through the Contract of Work along the southern coastline of Sumbawa. It also seems likely that a major NE-trending dextral fault runs up the bay directly west of Hu'u area (Fig. 1).

Deposit Geology

Early andesites

A volcanosedimentary sequence termed the Early andesites are the oldest rocks in the Onto project area and consist of a well-bedded sequence of mixed andesitic volcanic flows, volcanic breccia, and sills with local sedimentary interflow horizons. Major and trace element compositions of the Early andesites define a low-K calc-alkaline suite that ranges from basalt through andesite. This sequence is found around the margins of the drilled area in drill holes VHD050, VHD052, and VHD040 (Figs. 3, 4a). The sedimentary interflow horizons, which include bright red, laminated cherts, and hyaloclastic breccias, indicate that parts of this sequence formed in subaqueous, perhaps submarine conditions.

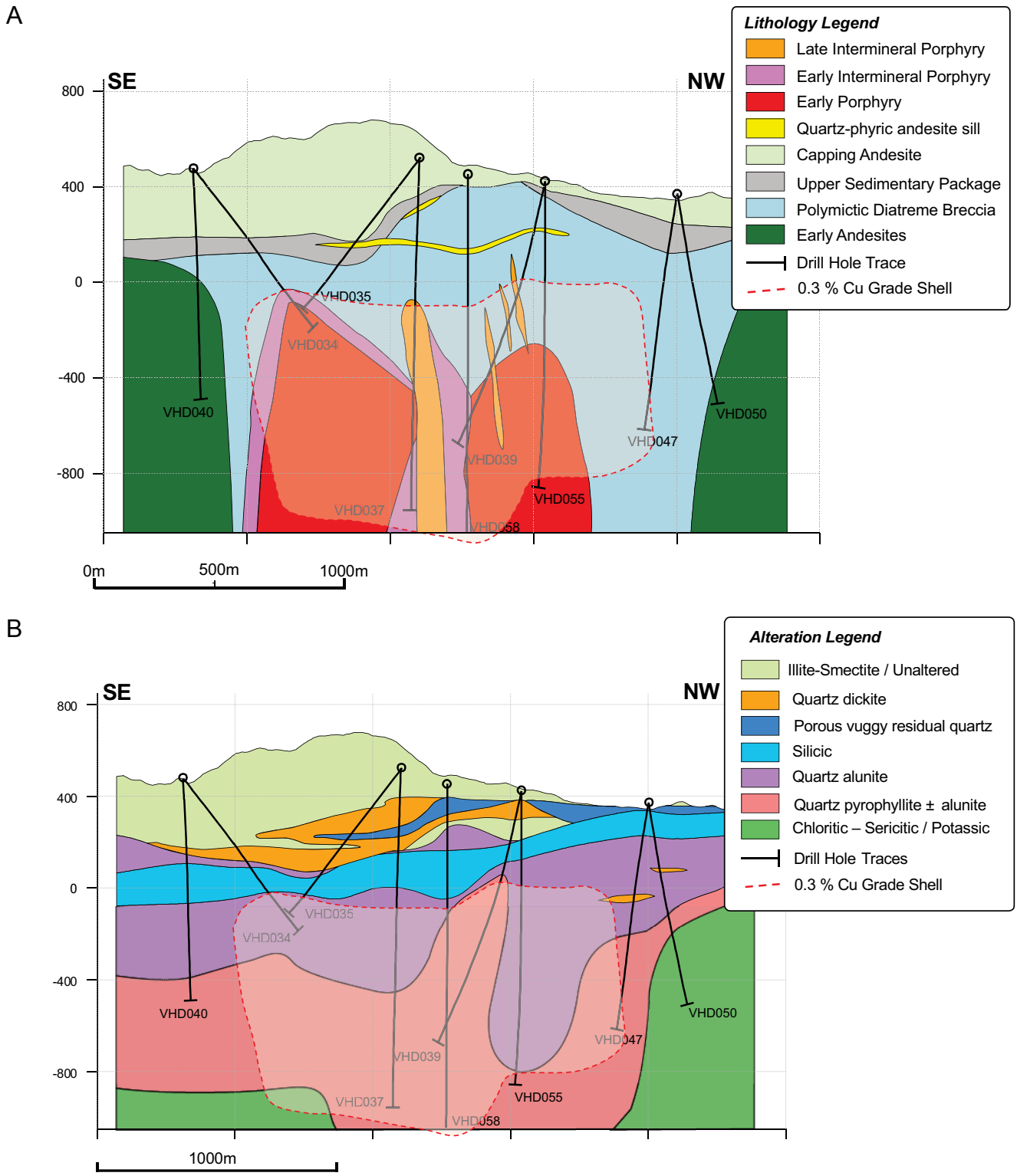

Fig. 4. SE-NW longitudinal section of a) lithology and b) alteration from Wadubura (drill holes VHD050 and 047) to Onto (drill hole VHD040). a) The andesites are thickest over the Onto area and thin toward Wadubura to the northwest. The Upper Sedimentary Package overlies and fringes the central polymictic (diatreme) breccia which is cored by porphyry intrusions from the early porphyry, to early intermineral porphyry to late intermineral porphyry. A late quartz-feldspar porphyry (QFP) sill is also shown in yellow, higher in the sequence. The 0.3% Cu cutoff shell is shown in dashed outline. b) Alteration, top to bottom, are unaltered to illite-smectite, down through quartz-dickite, which usually contains upper vuggy residual quartz (porous) horizon. A prominent, laterally extensive silicified vuggy-textured residual quartz alteration horizon (silicic) marks the top of the quartz-alunite and the quartz-alunite-pyrophyllite ± diaspore ± topaz alteration. Elevation is in meters relative to sea level (0 m).

Polymictic diatreme breccia

The main component of the volcanosedimentary package at Onto is a complex, matrix to clast-supported polymictic breccia, which is typically unbedded and poorly sorted over a vertical extent of at least 1,200 m (Fig. 4a). Rounded to subrounded clasts of porphyritic dacite and andesite predominate, but there are also fragments of siliceous sedimentary rocks, vuggy residual quartz, quartz-alunite clasts, pyritized sediment, and a variety of porphyry clasts (Fig. 5a, b), including a distinctive epidote-altered variety; in rare cases, there are magnetite-altered and A-veined porphyry clasts. Rare porphyry fragments with elongate and amoeboid forms with cuspate margins resemble juvenile fragments (Fig. 5c). Localized intercepts within the polymictic breccia are characterized by largely monomictic clasts dominated by eutaxitic-like textures that resemble flattened fiamme with subhorizontal to 60° attitude (Fig. 5d). Similar rock types also occur outside the northern margin of the diatreme vent in drill hole VHD052 (Fig. 3).

The polymictic breccia is interpreted to have formed in a diatreme vent to account for the polymictic nature of the fragmental unit, including juvenile fragments, lack of stratification, and the variable clast population (e.g., White and Ross, 2011). The outer limits of the diatreme have not been fully defined as it does not appear to crop out, but drilling suggests it is at least 2 × 1.5 km in extent with an estimated vertical thickness of at least 1,200 m, with several drill holes terminating in the breccia at depths of >1,000 to 1,523 m downhole.

Upper sedimentary package

The polymictic diatreme breccia is largely overlain by and is gradational into a bedded sedimentary sequence comprising laminated, locally carbonaceous, gray siltstones and tuffs, bedded polymictic breccias and volcaniclastic tuffs, and pyroclastic flows. The package ranges in thickness from 1 to 180 m (avg thickness, 50 m) currently over an area of 1.75 km (NW-SE) by 1 km (NE-SW) as defined by drilling. The sedimentary rocks in this package are finely laminated gray siltstones, varying from 0.5 to 92 m in thickness, with graded beds, and they display abundant soft-sediment deformation and undulating beds. They commonly contain volcanic bombs and layers of accretionary lapilli (Fig. 6), and were clearly formed in a subaqueous environment, most likely in a crater formed during the diatreme event. The volcaniclastic and pyroclastic units are not always present and seem to have variable thickness.

In a few diamond drill holes the pyroclastic tuffs are up to 75 m thick and are similar to the pyroclastic units observed within or at the margins of the underlying polymictic breccia with lithic fragments and fiamme-like fragments. Bedded polymictic breccia layers sometimes define the base of the upper sedimentary package and are gradational into the diatreme. They are similar to the diatreme breccia in terms

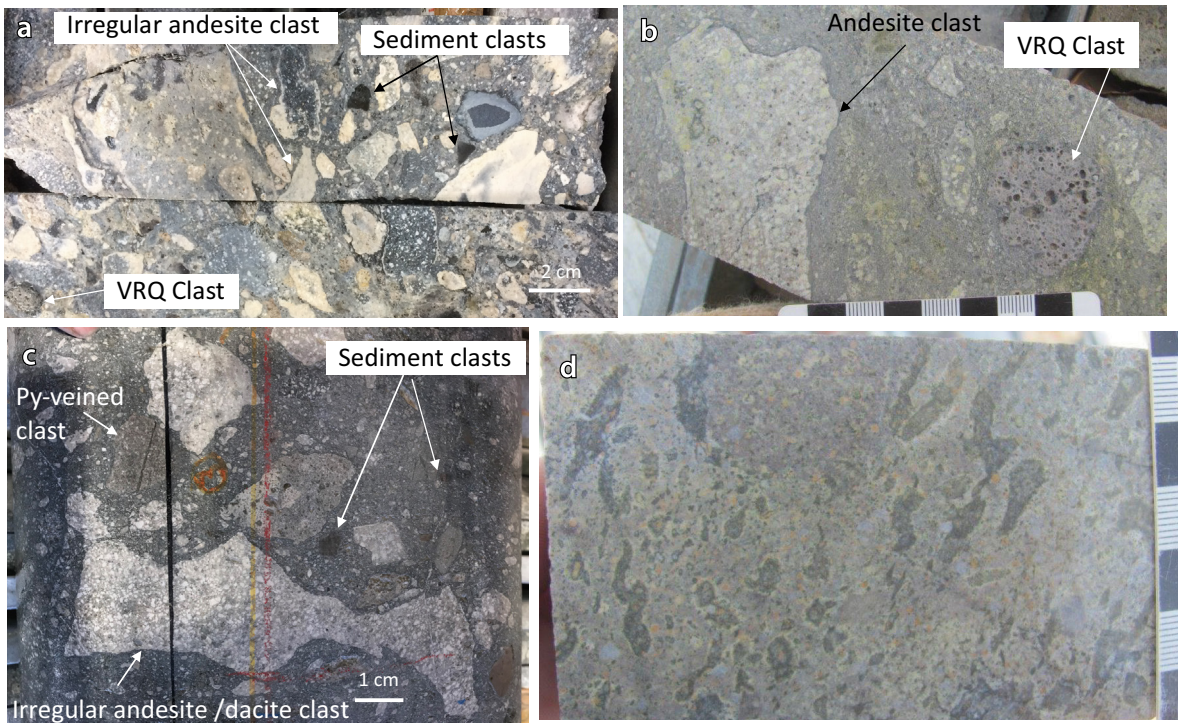

Fig. 5. Polymictic diatreme breccias from Onto. a) VHD088, interval 105-106 m, variable unsorted polymictic breccia typical of the upper parts with irregular clasts of andesite to dacite porphyry, fine-grained bleached and dark pyritic sedimentary rock, and some vuggy residual quartz clasts (extreme bottom left). Many clasts also have alteration rims. b) VHD044-209.5 m, clast of vuggy residual quartz in polymictic breccia with clasts of andesite, many with irregular shapes; c) VHD089-80.5 m, highly irregular dacite clast with cuspate margins, interpreted as juvenile fragments, in polymictic breccia. Variable clasts of andesite, dacite, and dark sedimentary rock. Note also pyrite-veined clast just left of black line and clasts within clast in center of photo. d) VHD045, interval 410-422 m, pyroclastic interval within polymictic breccia with lithic clasts in dacitic matrix with quartz phenocrysts. The lithic clasts are irregular and elongate, indicating that they were plastic during deposition; interpreted as juvenile clasts.

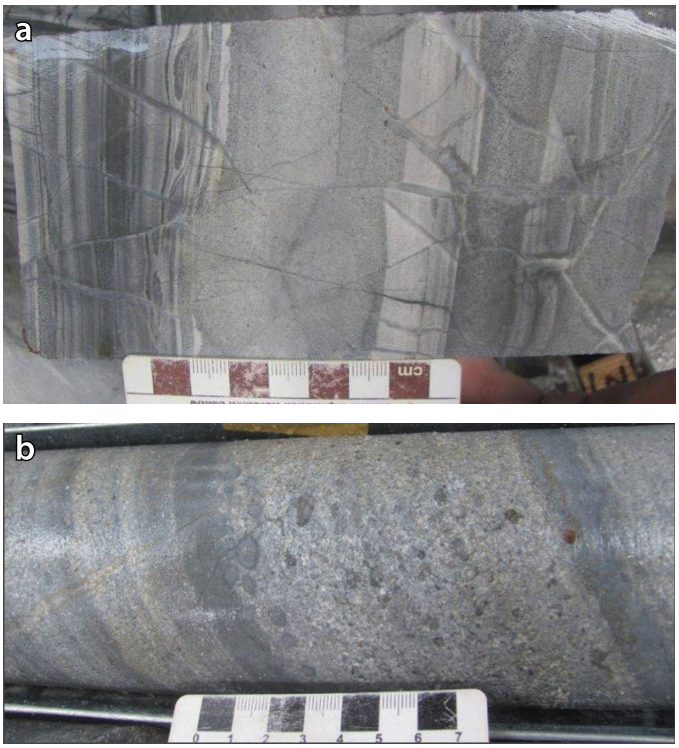

Fig 6. Representative photographs showing upper sedimentary package at Onto. a) VHD040-346.5 m, laminated siltstone with graded bedding; b) VHD042-276.7 m, accretionary lapilli in well-laminated tuffaceous sediments and siltstones.

of clast type and abundance but display coarse layering and more variable clast compositions, the base of the sedimentary package being taken at the last recognizable sedimentary layers.

Capping andesite

The upper sedimentary package is capped by a relatively unaltered andesite that forms most of the higher ground around Onto. In drilling, it is generally 300 to 400 m thick in the central Onto area but is partially eroded going farther to the northwest in the Wadubura area (Fig. 4a). The andesite is a phenocryst-rich porphyritic andesite with large, fresh plagioclase and hornblende phenocrysts and primary magnetite. Only rarely are quartz phenocrysts present.

A few minor beds are observed but in general it is relatively uniform and massive without flow foliations or flow-aligned phenocrysts. The andesite is interpreted to form in flow domes with talus breccias around the edges with a roughly planar lower contact (Fig. 4a). The capping andesites are low-K andesites in composition based on major elements. The andesite very locally contains rounded xenoliths of magnetite-rich rock.

Phreatic breccia

The capping andesites and the upper sediments are injected in places by small steep, anastomosing, phreatic breccia dikes or pipes, characterized by rock-flour matrix. Several are localized by fault zones. The fragments are mainly from the surrounding andesite, although in some cases they also contain possible sedimentary fragments and vuggy residual quartz fragments with rare covellite, suggesting late timing and origin from below the andesite flows. The phreatic breccias are generally weakly anomalous in copper (150–500 ppm) with variable arsenic (10–100 ppm) and gold (0.02–0.03 ppm).

Multiphase porphyry intrusions

The polymictic diatreme breccia was intruded by a series of porphyry stocks up to about 50 m below sea level (bsl), corresponding to 500 to 600 m below the current surface (Fig. 4a). The stocks coalesce into a composite NW-trending intrusion that is 1.6 × 0.6 km at 500 m bsl, expanding to 1.8 × 0.8 km at 1,000 m bsl. The subdivision of the porphyry phases is complicated by textural destruction due to the pervasive advanced argillic alteration and even drill cores with relict igneous porphyritic textures are intensely altered and composed of 40 to 60% quartz, 10 to 40% alunite, 5 to 20% pyrite ± pyrophyllite and diaspore. It is possible, however, to divide the intrusions into three phases (early porphyry, early intermineral, and late intermineral) based on preservation of porphyritic textures, intensity of alteration, quartz flooding, and intensity of A- and B-type quartz veinlets. Independent evidence for porphyry contacts is also observed locally as xenoliths of early quartz-veined porphyry clasts, or floating quartz veinlet xenoliths in the younger porphyry phases close to contact with older phases (Fig. 7a, b). More rarely, veinlets are truncated at the contacts.

The subdivision of the porphyry stocks is important in the geologic model and understanding grade distribution, as despite the degree of alteration, the copper and gold contents generally become progressively lower from the oldest to the youngest. The early porphyry carries grades of ~1.2% Cu and 0.7 g/t Au where quartz veinlet stockworks are well developed, typically over a ~350-m interval between 450 and 1,000 m bsl while the average grades of the early intermineral and late intermineral porphyries are 0.8% Cu and 0.38 g/t Au, and 0.6% Cu and 0.28 g/t Au, respectively.

Early porphyry

The early porphyry occurs as a series of small (<200 m in cross section) vertical stocks that top out at about the 50 m bsl but appear to increase and perhaps coalesce at depth at ~1,000 m bsl. The early porphyry commonly shows irregular wavy, wormy-textured (gusano) A-type quartz veinlets (Fig. 7c) typical of the apical portions of porphyry stocks (Gustafson et al., 2004; Sillitoe, 2010). The early porphyry has highest magnetite (now hematite where advanced argillically altered) and A and B quartz veinlet stockwork intensity commonly >30% quartz veinlets (Fig. 7d). Some of the higher-grade mineralization (≥1% Cu, ≥1 g/t Au, Cu/Au ~1:1) is associated with these stockworks at the top of the stocks, with high quartz vein densities, such that up to >50 to 90% of the rock consists of veins (Figs. 7d-f).

Early intermineral porphyry

The early porphyry stocks are cut by early intermineral porphyry intrusions characterized by intervals with >15 B veinlets in a 5-m interval but generally lacking the intense fine magnetite and A-B quartz veinlet stockworks (Fig. 7f). Like the early porphyry, the early intermineral porphyry occurs as

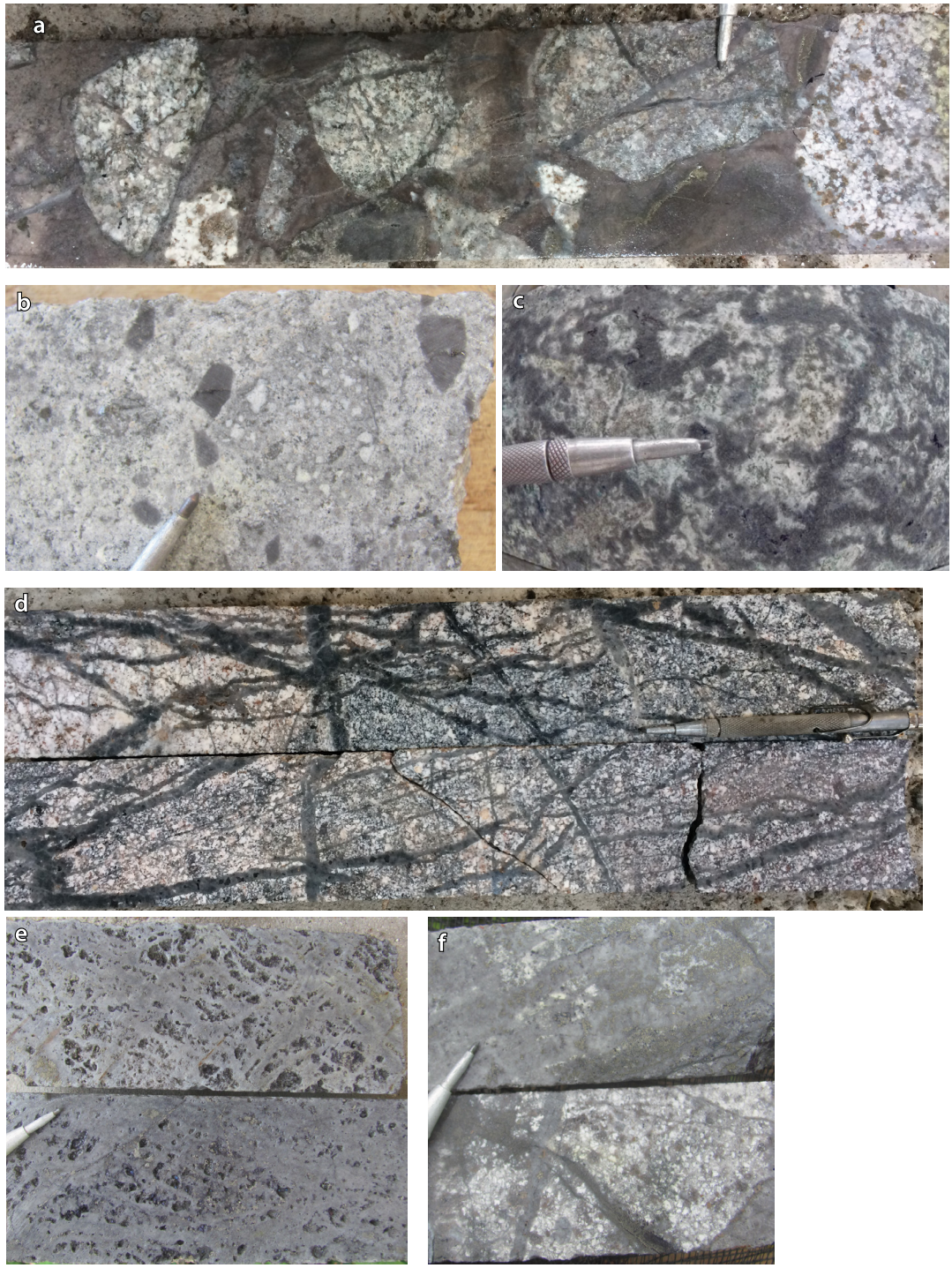

Fig 7. Examples of the three main porphyry intrusion phases and their contact zones from Onto. All examples are from quartz-alunite alteration zones except for the one shown in f, which is hosted in quartz-pyrophyllite-diaspore-alunite alteration. a) VHD088-593 m (–102 m RL) A-B quartz veined early intermineral porphyry fragments in the late intermineral porphyry at contact. Contact zone also contains quartz vein xenoliths. b) VHD076-900 m (–302 m RL), "floating" quartz vein xenoliths in a late intermineral porphyry close to the contact with the early porphyry higher in the hole. c) VHD044-721 m (–288 m RL), wormy-textured A-type quartz veinlets at apex of early intermineral porphyry. d) VHD087, interval 815 to 816 m (–138 m RL), A-B–type quartz veinlet stockwork in the early porphyry. 1.1% Cu, 0.92 g/t Au and 9 ppm As with 8% sulfur, 2-m interval. e) VHD076-765 m (–190 m RL) >80% A and B veins in early porphyry overprinted by strong leaching that has removed most of wall rock between quartz veins; 2.5% Cu, 1.6 g/t Au, and 11% S with only ~1% Al_2O_3. f) VHD058–1,238.5 m (–785 m RL) and 1,228.1 m (–775 m RL) (lower piece), early porphyry (upper) shows irregular A- and B-type gray quartz veins with porphyritic texture largely destroyed by quartz flooding; lower piece of core is early intermineral porphyry with less A veins and more prominent B veins, but with recognizable porphyry texture. See Figure 3 for drill hole location. RL = elevation relative to sea level.

vertical stocks (~200–300 m in diameter) and also commonly shows irregular wavy, wormy-textured (gusano) A-type quartz veinlets typical of the apical portions of porphyry stocks. The matrix is often strongly altered and quartz flooded, but plagioclase porphyritic textures are sometimes preserved. Within 2 to 4 m of contact with early porphyry, it is common to see quartz vein xenoliths floating in and partially assimilated by this later intrusion. The early intermineral porphyry has typical grades of ~0.6 to 0.8% Cu and 0.2 to 0.4 g/t Au and a narrow range of Cu/Au ratios of about 3:1. The early intermineral porphyries also top out at ~50 m bsl, some 500 to 600 m below the current surface.

Late intermineral porphyry

The late intermineral porphyry is a plagioclase-hornblende phyric intrusion with sparse B veins, with one to 10 B veins in 5-m intervals, but in many cases B-type quartz veinlets are absent. Igneous textures can be well preserved and quartz flooding/textural obliteration is rare. It is also common to see xenoliths of rock and quartz veinlets from earlier porphyries along its contacts (Fig. 7a, b). The late intermineral porphyry has typical grades of ~0.4 to 0.6% Cu and 0.1 to 0.3 g/t Au; however, high Cu grades are related to late veins of pyrite-covellite. The late intermineral porphyry has a characteristic Cu/Au ratio of ~3:1. The contacts with earlier intrusions and wall rock often have low- to moderate-angle contacts suggesting intrusion as sills and dikes rather than as pencil-shaped intrusions like the two earlier porphyry phases. The late intermineral porphyry has been intersected as high up as 25 m bsl.

Later intrusions

Two additional intrusions observed at Onto are plagioclase ± hornblende andesite dikes and quartz-phyric andesitic to dacitic flat-lying sills (less commonly dikes) usually within or close to the base of the upper sedimentary package or high in the polymictic breccia unit. The andesite dikes may be feeder dikes to the overlying capping andesite flow domes.

The sills are consistently present and are observed over a strike length of at least 1 km (Fig. 4a). Both intrusion types are difficult to recognize through the advanced argillic alteration but quartz eyes in the sills are preserved through even the most intense advanced argillic alteration. These intrusions lack any A or B veins, but do contain high sulfidation–style pyrite. The dikes in particular are often less altered (smectite or argillic) than the surrounding rocks, indicating they may postdate some of the subsequent advanced argillic alteration.

Alteration

The Onto deposit occurs within remnants of a large lithocap covering at least 30 km^2, but this manuscript only describes hydrothermal alteration in the immediate area of the Onto deposit discovery. At Onto, drilling has outlined a broadly subhorizonal geometry within the lithocap alteration. The alteration is described below from top to bottom, starting in illite-smectite and going down progressively through quartz-kaolinite, quartz-dickite, two separate vuggy residual quartz horizons, quartz-alunite, and lowermost quartz-pyrophyllite ± diaspore alteration zones (Figs. 4b, 8).

Only a few holes pass through the base or side of the margins of the advanced argillic alteration package and into biotite-magnetite and/or chlorite-muscovite alteration. These porphyry-related alteration types are described separately.

Lithocap Alteration

Drill core logging at Onto, supplemented by short wave infrared (SWIR) spectroscopy of samples at 0.5 to 1.0 m intervals with on-site ASD instruments, has defined a remarkably thick zone of intense advanced argillic alteration, over an area of at least 1.5 × 1.0 km with a thickness of >1,200 m in the central portion, where several of the deeper holes (e.g., VHD037 and VHD045) bottom in advanced argillic alteration at 1,500 m downhole (Figs. 4b, 8). This alteration is well developed in the polymictic breccia but also occurs within all the intrusion types and also, to a limited extent, in the early andesites, but less intensely. The lithocap thins around the edges of the current drilling (e.g., VHD038 ~1 km out from core of system; Fig. 3) but even here is between 400 and 500 m thick.

Illite-smectite/unaltered

Most of the capping andesite flows are essentially unaltered, with the original Na_2O values ≥2% preserved along with Ba (>400 ppm), relatively high Sr >250 ppm, V >100 ppm and sulfur values are also generally ≤4%. In the lower portions, the andesite lava flows become increasingly altered with illite-smectite alteration, first in fractures and then pervasively, by a light green-colored smectite (montmorillonite in ASD) alteration with illite.

In a few peripheral drill holes at Onto, illite-smectite alteration in fractures is observed to overprint chlorite and chlorite-epidote alteration, interpreted as regional alteration (see discussion of propylitic alteration below). Illite-smectite alteration zones also consistently occur deeper in some areas, below quartz-dickite alteration (Figs. 4b, 8).

Quartz-dickite

Dickite-dominated alteration zones with kaolinite ± pyrophyllite form a discontinuous 100-m-thick zone at the top of the advanced argillic alteration interspersed with smectite-dominated alteration zones, indicating the fluid responsible became both cooler and less acidic upward into the capping andesite. Very occasionally, at the edges of the system (e.g., VHD049, see Fig. 3) quartz-dickite alteration clearly overprints illite-smectite alteration in subhorizontal fractures before more pervasively altering the rock.

Porous vuggy residual quartz

A 10- to 80-m-thick subhorizontal porous to friable vuggy quartz horizon typically occurs within or toward the base of the quartz-dickite alteration, corresponding roughly to the base of the capping andesite and also to the current position of the groundwater table at 180 to 200 m asl (Figs. 4b, 8). It is characterized by porous to friable silica commonly with abundant dark, fine-grained pyrite. Vuggy quartz textures are well developed when in the capping andesites (Fig. 9a), but are often more porous and friable when developed in the upper sedimentary package or in the top of the polymictic breccia. It is normally aspectral in ASD or has water-silica and lacks alunite (Fig. 8). To the northwest, at Wadubura (Figs. 4b, 8),

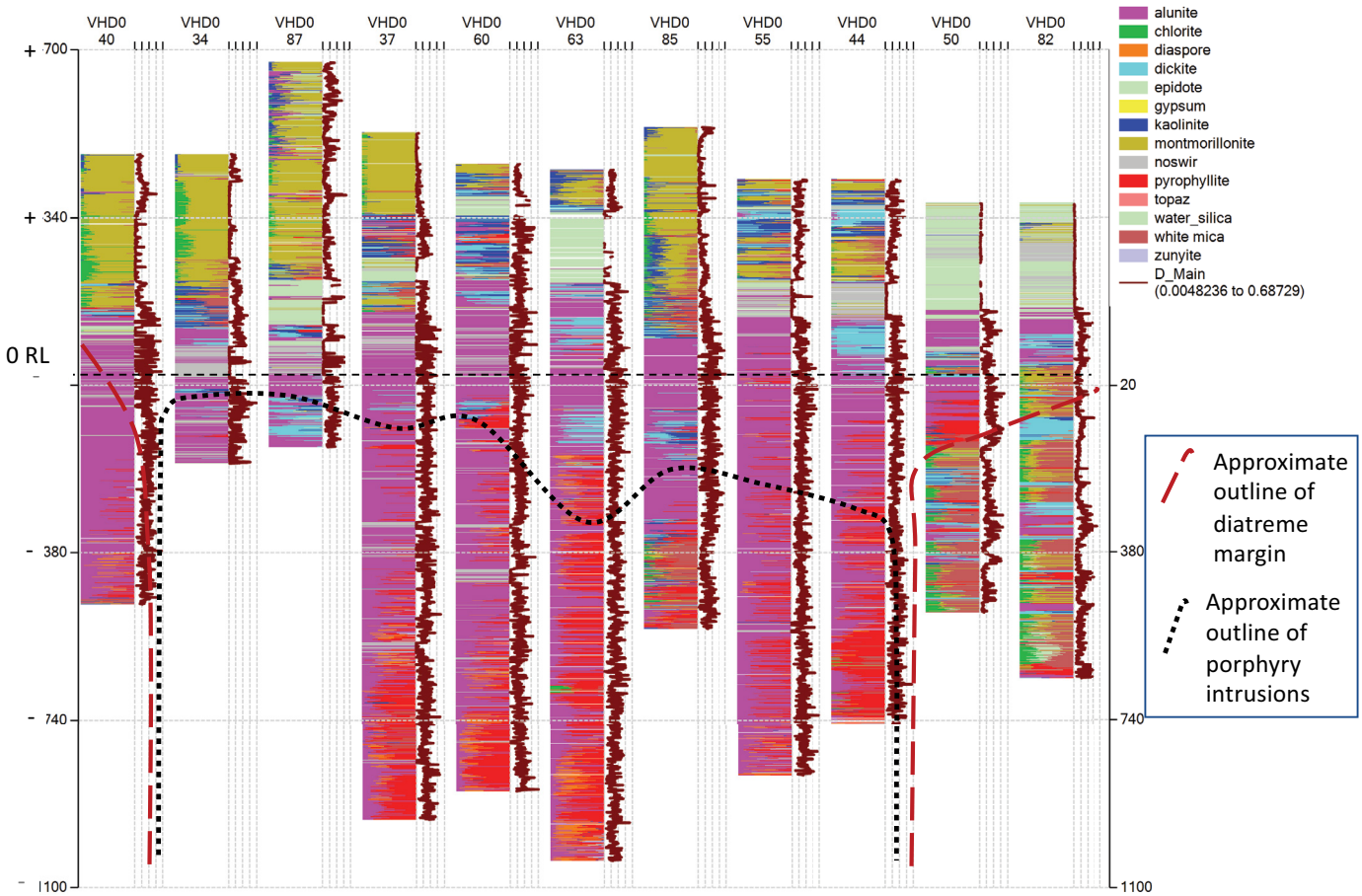

Fig. 8. Drill holes along SE-NW longitudinal section (as in Fig. 4b) arranged in pseudo-section showing relative spectral contribution from short wave infrared (SWIR) spectroscopy of samples at 1-m intervals with on-site ASD instruments. Plotted in aiSIRIS™ software provided by AusSpec. The approximate margins of the diatreme breccia and the porphyry intrusions are shown for reference.

where erosion has cut a valley down into the alteration system, this alteration extends to surface. Here, bleached spongy white silica-kaolinite-sulfur ± alunite alteration appears to have overprinted a portion of the outcropping earlier quartz-dickite-kaolinite and vuggy residual quartz alteration.

Silicic

The top of a much more pervasive and intense quartz-alunite to quartz-pyrophyllite alteration zone is always marked by a gently dipping, subhorizontal horizon of vuggy residual quartz and silicification. In most holes, particularly to the southeast, silicification is complete but occasionally vuggy textures remain, indicating silicification overprinted a vuggy residual quartz horizon that developed before silicification (Fig. 9b). The majority is, however, a massive silicified rock so it has been referred to as the "silicic" horizon.

This horizon is consistently developed over a 100- to 200-m-wide interval, occasionally up to 300 m, at about sea level elevation. ASD readings are aspectral, show water-silica (water in fluid inclusions in quartz) or indicate K-alunite (with alunite absorption peak at ~1,476 nm). This zone is a useful marker and occurs in nearly all holes drilled to date and normally has very sharp upper and lower contacts. The silicic alteration horizon is characterized by <1% Al_2O_3 (commonly <0.5% Al_2O_3) and intense leaching of most elements, including Ti and Zr, indicative of low pH fluids that dissolve everything but quartz and pyrite. Hydrothermal monazite and zircon are observed. Vuggy quartz zones commonly develop with quartz-alunite alteration lower down in the sequence but always without the extreme Al depletion—usually >2 to 9% Al_2O_3.

Quartz-alunite

Below the silicic horizon, quartz-alunite with subordinate pyrophyllite occurs over wide continuous intervals (Figs. 4b, 8). Thin intervals of this alteration are also present in places above the silicic horizon. The quartz-alunite is light-colored alteration with patchy texture where dickite, alunite, and pyrophyllite preferentially replace the clasts in the polymictic breccia (Fig. 9c). Lilac blue dumortierite occurs sporadically, locally up to 5% by volume, though it also occurs in the quartz-pyrophyllite ± diaspore described below. Dumortierite usually occurs within the polymictic breccia within a few hundred meters of the porphyry intrusions. Quartz-alunite alteration commonly overprints the higher temperature quartz-pyrophyllite ± diaspore alteration and is generally more porous with a greater proportion of vuggy-textured residual quartz developed in subhorizontal zones and less commonly in steep

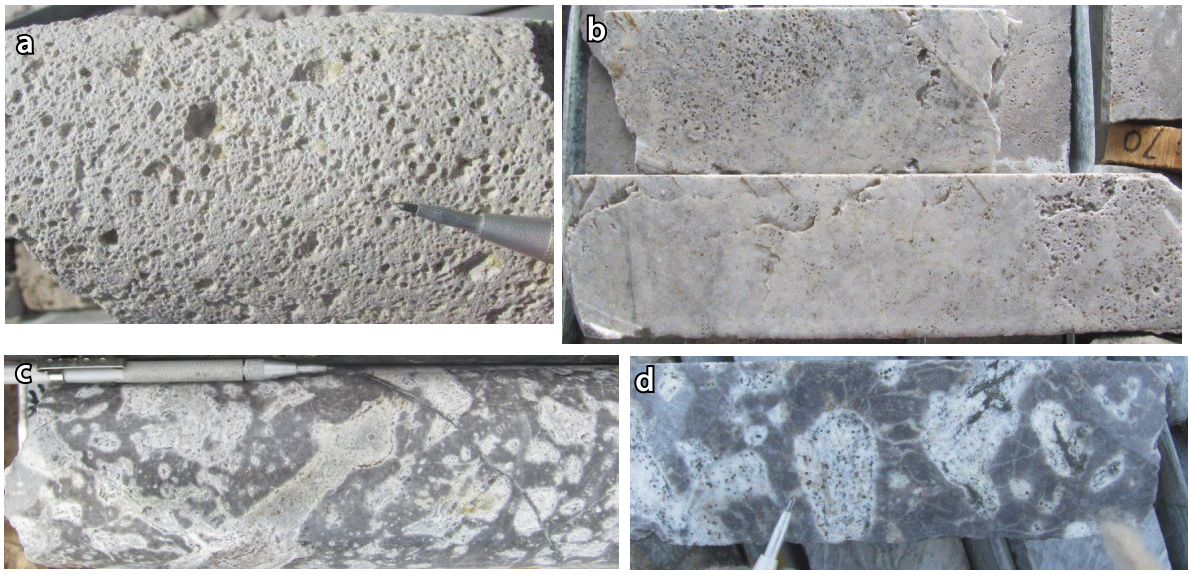

Fig. 9. Typical advanced argillic alteration types at Onto. a) VHD047 at 23 m, porous vuggy quartz alteration in massive capping andesite with vugs after plagioclase and amphibole; 0.42% Al_2O_3, 2.9% S, and 5 ppm Cu. b) VHD041, interval 492–494 m, samples of vuggy residual quartz from margin of Silicic alteration zone with silicification overprinting vuggy textures; 0.98% Al_2O_3 with 0.3% S and 47 ppm Cu. HQ cores are 63.5 mm across. c) VHD078 at 585 m, quartz K-alunite alteration with patchy ragged textures in polymictic breccia 5.7% Al_2O_3 with 0.16% Cu. d) VHD046 at 656 m, patchy amoeboid to ovoidal textures in resorbed fragments in polymictic breccia within early, high-temperature alteration with Na-alunite-pyrophyllite ± topaz and dumortierite alteration.

to vertical zones. The quartz alunite alteration domain is characterized by Al_2O_3 concentrations from <10 to ~6.5 wt %; lower values reflect localized vuggy-textured residual quartz development as leaching and/or quartz flooding intensifies.

Quartz-pyrophyllite ± diaspore

The deepest (generally ≥400 m bsl) and highest temperature advanced argillic alteration is characterized by an assemblage of quartz-pyrophyllite with diaspore and variable amounts of alunite, topaz, zunyite, dumortierite, Na-alunite, and pyrite (Figs. 4b, 8). Petrography also indicates corundum and andalusite. In the drill core, this alteration type is very distinctive with a compact brownish to tan-colored matrix with pyrophyllite and/or diaspore with ragged, whitish patchy to ovoid textures representing resorbed and modified clasts (Fig. 9d). Quartz-pyrophyllite dominates in the top portion and diaspore with topaz and zunyite gradually becoming more abundant, generally below ~600 m bsl (Fig. 8). The quartz-pyrophyllite ± diaspore alteration is commonly preserved at much higher levels (75–470 m bsl), to as high as 6 m asl. The overprint boundary of earlier high-temperature alteration with later quartz-alunite is often transitional rather than sharp and in many cases the alteration is a mixture of the two types.

Porphyry-Style Alteration

Potassic

Potassic alteration is occasionally identified by the presence of hydrothermal magnetite and biotite ± K-feldspar. It is indicated in ASD by Fe-Mg chlorite, paragonite, and muscovite with lesser amounts of alunite, but commonly there is a weak quartz-alunite, quartz-dickite, and/or quartz-kaolinite overprint. Relict blocks of potassic or chloritic alteration are sometimes observed within quartz-alunite and quartz-pyrophyllite-diaspore alunite alteration surrounded by hematite (martite) after disseminated or veinlet magnetite. Potassic alteration, where recognizable, is usually overprinted by chloritic alteration to varying degrees. Relict potassic alteration has only been recognized in the very bottom of a few holes (e.g. VHD044 and VHD080) and in VHD062R between 738 and 1,090 m marginal to the advanced argillic-altered package (Fig. 3). A- and B-type quartz veinlets, which form with high-temperature potassic alteration in many porphyry copper deposits, are widespread at Onto over intervals of 300 to 400 m.

Phyllic-chloritic

This alteration is characterized by muscovite (sericite)-quartz ± chlorite alteration, commonly with pyrite at the base of several holes, most noticeably in VHD036, VHD049, and VHD053. Phyllic-chloritic alteration is rarely very extensive and it is common to see a weak argillic or weak quartz-dickite overprint. This alteration often appears to be overprinting potassic alteration that is indicated by remnant magnetite. It occurs more commonly in the early porphyry and early intermineral porphyry and rarely in the late intermineral porphyry and polymictic breccia wall rock.

Propylitic

A propylitic alteration assemblage of chlorite-epidote-calcite ± actinolite is observed in the base of several early holes (VHD033, VHD038, and VHD050), usually as relict alteration in less permeable lithologies, and was originally thought to be propylitic alteration related to the porphyry intrusions. More recently, drill holes to the north of Onto, laterally

outside the advanced argillic alteration, typically pass through illite-smectite to chlorite to chlorite-epidote alteration at depth, indicating that chlorite-epidote alteration likely forms during regional alteration from near-neutral pH fluids.

Mineralization

The first sign of copper-gold mineralization is a distinct zone of Ag-As-Sb-Bi ± minor Cu and Au enrichment toward the base of the silicic alteration horizon. This zone is associated with fracturing of the base of the silicic horizon and introduction of fine-grained dark pyrite. In the southeastern extent of the deposit this zone directly caps the main covellite-pyrite–dominated copper-gold mineralization that starts in the quartz-alunite alteration directly under the silicic zone at approximately sea level, between 300 and 600 m below surface. At the northwestern extent of mineralization at Wadubura, copper-gold mineralization, as defined by the 0.3% Cu grade shell, is ~150 m below the basal contact of the silicic horizon, as the silicic horizon dips shallowly to the southeast (Fig. 4b). Many drill holes terminate in mineralization at 1,200 to 1,500 m downhole, corresponding to ~800 m bsl. Typical mineralized intervals in drill core are listed in Table 1. Two main mineralization types are apparent, intense A-B quartz veinlet related to porphyry stocks apparently represent the porphyry environment and sulfides with high-sulfidation states that are more typical of the lithocap environment. There is, however, unlike many linked porphyry high-sulfidation epithermal systems, a complete spatial overlap, and perhaps temporal overlap between the two styles.

Chalcopyrite-bornite related to biotite-magnetite alteration

On the margins (e.g., in VHD062R; Fig. 3) and in rare cases, below the base of the advanced argillic alteration, the early porphyry and early intermineral porphyry have low- to intermediate-sulfidation assemblages of chalcopyrite ± pyrite ± bornite ± digenite/chalcocite associated with magnetite and hydrothermal biotite alteration, plus A- and B-type quartz veinlet stockworks (Fig. 10a). Grades in the early porphyry are variable but generally ~1% Cu and ~1 g/t Au, with gold grades >1 g/t typically associated with intervals of bornite. Chalcopyrite-bornite mineralization has very low arsenic values. For example, the early porphyry intersection in potassic alteration in VHD062R grades 0.93% Cu, 1.34 g/t Au, and 44 ppm As with 5.3% S, while the most pristine intervals with little advanced argillic overprint average only 8 ppm As and 3% S. In the same hole, the early intermineral porphyry with potassic alteration grades ~0.53% Cu, 0.23 g/t Au, 7 ppm As, and 3.8% S. Chalcopyrite-bornite ± pyrite mineralization makes up a small proportion (~8%) of the resource drilled to date at Onto.

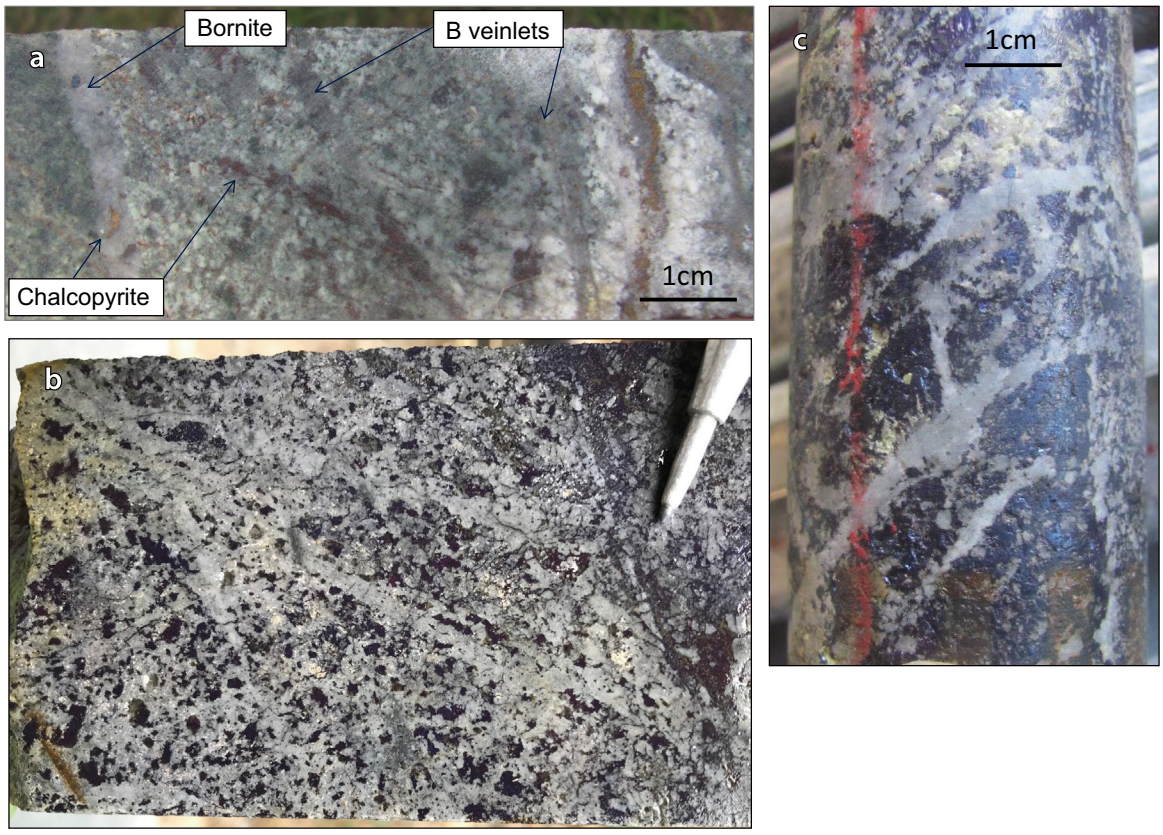

Fig. 10. Mineralization in the early porphyry. a) VHD 062R-993 m, early porphyry with intense magnetite and A vein stockwork with B veins in potassic alteration with magnetite-chalcopyrite ± bornite internal clots in veinlets; 1.1% Cu, 3.3 g/t Au and 7 ppm As with 2.4% S over 2 m. b) VHD086-699 m, Intense A veinlet quartz stockwork with coarse covellite interstitial to veins as rock is dissolved. 12.7% Cu and 2.33 g/t Au, 2-m interval. c) VHD063–1,083 m, early porphyry with dense quartz vein stockwork with interstitial covellite probably after chalcopyrite ± bornite. 16.3% Cu and 4.2 g/t Au with 397 ppm As, 2-m interval.

High-sulfidation mineralization

With the rare exceptions noted above, copper-gold mineralization at Onto is typified by a high-sulfidation assemblage of covellite-pyrite ± native sulfur with very minor enargite associated with quartz-alunite-pyrophyllite–dominated alteration. The covellite defines a very high sulfidation state (Einaudi et al., 2003) with digenite and chalcocite present only in trace amounts. Nukundamite is also observed intergrown with both pyrite and covellite (Fig. 11g). Nukundamite is stable at temperatures between 501° and 223°C at very high sulfidation states at higher values of f_{S_2} and f_{O_2} than chalcopyrite + bornite and chalcopyrite + pyrite, assemblages (Inan and Einaudi, 2002). Barite is also common in the upper portions of the mineralized zone.

Just over 90% of the current resource occurs in the quartz-pyrophyllite-alunite and quartz-alunite alteration with bulk mineralogy of the mineralization at 0.3% cutoff approximately 50 to 60% quartz, 5 to 15% alunite, and 10 to 25% pyrite with up to 5% pyrophyllite, dickite, and kaolinite with a few percent covellite. Average sulfur and iron values in the mineralized resource are 11% S and 9% Fe.

Covellite and pyrite are typically late relative to quartz and alunite; covellite often grows into open space (Figs. 10b, c, 11a,

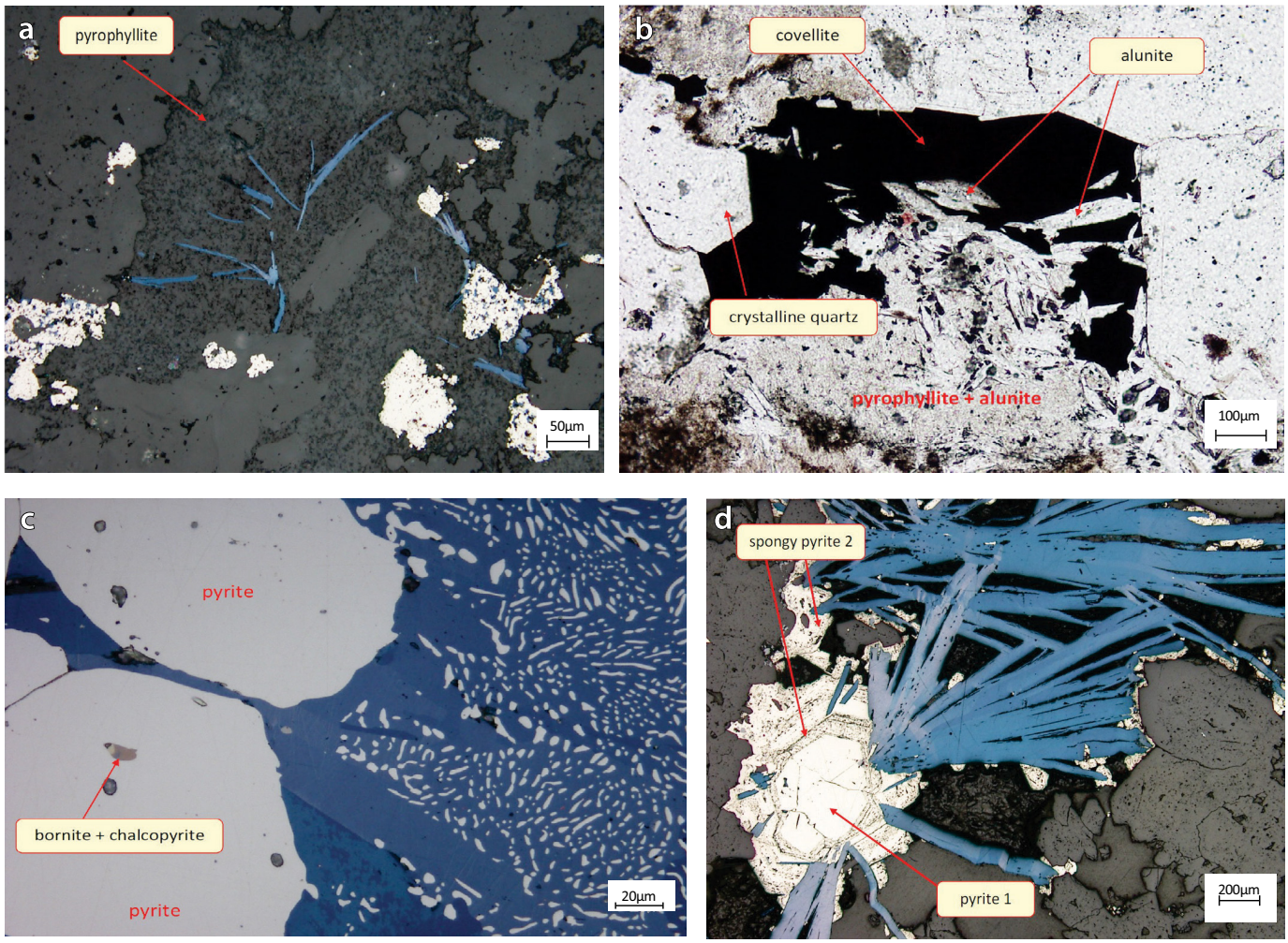

Fig. 11. Reflected light photomicrographs (unless otherwise noted). a) VHD039–845.7 m, bladed covellite in aggregate of pyrophyllite which may infill cavity and replace kaolinite. Pyrite (bottom left) riddled with covellite. Gray elongate grains below covellite are alunite and round quartz (scale bar 50 μm). b) VHD037–1,037.6 m, covellite in early porphyry within quartz-pyrophyllite-alunite alteration. Hypogene covellite in cavity with crystalline quartz; alunite included in and intergrown with the covellite. Finer crystals at bottom are mixed alunite and pyrophyllite (scale bar 100 μm; plane polarized light). c) VHD037–1,150 m, intergrown covellite and pyrite on margin of irregular A vein in early porphyry within quartz-pyrophyllite-alunite ± diaspore-zunyite alteration. This photomicrograph shows the "myrmekite-like" or vermicular texture of pyrite within covellite, suggesting an increase in sulfur fugacity with chalcopyrite (or fukuchilite) being replaced by covellite + pyrite (Teale, pers. commun., 2015). Note the small bornite + chalcopyrite inclusion within pyrite. Scale bar 20 μm. d) VHD045–1,103.5 m, bladed covellite and two generations of pyrite fill open space. Covellite nucleates on earlier pyrite but cuts and/or intergrown with spongy type 2 pyrite; gray mainly quartz. Pyrite 1, inclusion free and idioblastic, is rimmed by inclusion-choked "spongy" pyrite 2 with covellite inclusions <10 μm in size; pyrite 2 also hosts coarse enargite inclusions. Covellite blades are intergrown with elongate alunite crystals. Early intermineral porphyry with moderate quartz stockwork in quartz alunite-pyrophyllite alteration (scale bar 200 μm). Mineragraphic, petrological, and SEM investigations of drill core samples was undertaken by Graham Teale (Teale & Associates Pty Ltd.) and provided in reports to Vale in 2014 and 2015.

b) but is also commonly intergrown with and/or overgrown by with quartz, alunite, and native sulfur (Figs. 11b, 12c, d). Covellite is also intergrown with a late (stage 2) spongy, growth-banded pyrite that overgrows cores on inclusion-free stage 1 pyrite (Fig. 11d). In rare cases it possible to discern quartz-alunite halos on pyrite-covellite veins, indicating these veins formed at same time as quartz-alunite alteration (Fig. 12b).

Early-stage geometallurgical studies indicate two-thirds of the gold occurs as small inclusions in pyrite > covellite, with the remaining third as structural (lattice) gold in pyrite >> covellite. Silver in contrast occurs mainly as matildite ($AgBiS_2$), with ~25% contained in lattice sites in enargite and pyrite. Typically, in high-sulfidation deposits, the spongy stage 2 pyrite (Fig. 11d) is arsenian pyrite and carries gold where the early pyrite crystallizes with enargite under more reduced conditions (Deditius et al., 2008), but this has not been verified at Onto to date.

High- to very high sulfidation mineralization includes the following:

1. Fine- to locally coarse grained disseminated covellite-pyrite within the porphyry intrusions and polymictic breccia. In the early porphyry intrusion in particular, covellite occurs with only minor pyrite as coarse (several mm) crystals and rosettes, replacing the original wall rock between the veins and to a lesser extent as disseminated covellite within the quartz veinlets (Figs. 7e, 10b, c). Covellite is intergrown with pyrophyllite, alunite, dickite, pyrite, native sulfur and, more rarely, anhydrite (Fig. 11a, b). There is complete fine-scale replacement of all preexisting copper sulfides by covellite-pyrite. Chalcopyrite and bornite ± chalcocite are preserved only in the A-B quartz veinlets as rare micro-inclusions within pyrite, in covellite, or encapsulated within quartz (Fig. 11c).
2. Covellite-pyrite-native sulfur fills vugs in quartz-alunite alteration zones as original minerals are leached out during alteration and vuggy quartz textures develop. Coarse vugs also develop as alunite and pyrophyllite become unstable in late fluids and are leached out, forming a highly permeable rock that is infilled sequentially with pyrite, covellite, and native sulfur (Fig. 12a). Pyrite-covellite veins are locally observed with quartz-alunite alteration halos, indicating mineralization formed with quartz-alunite alteration (Fig. 12b). The covellite is typically coarse and crystalline and commonly intergrown with pyrite but also with native sulfur and alunite, and more rarely with dickite in open-space fillings (Figs. 11, 12c, d).

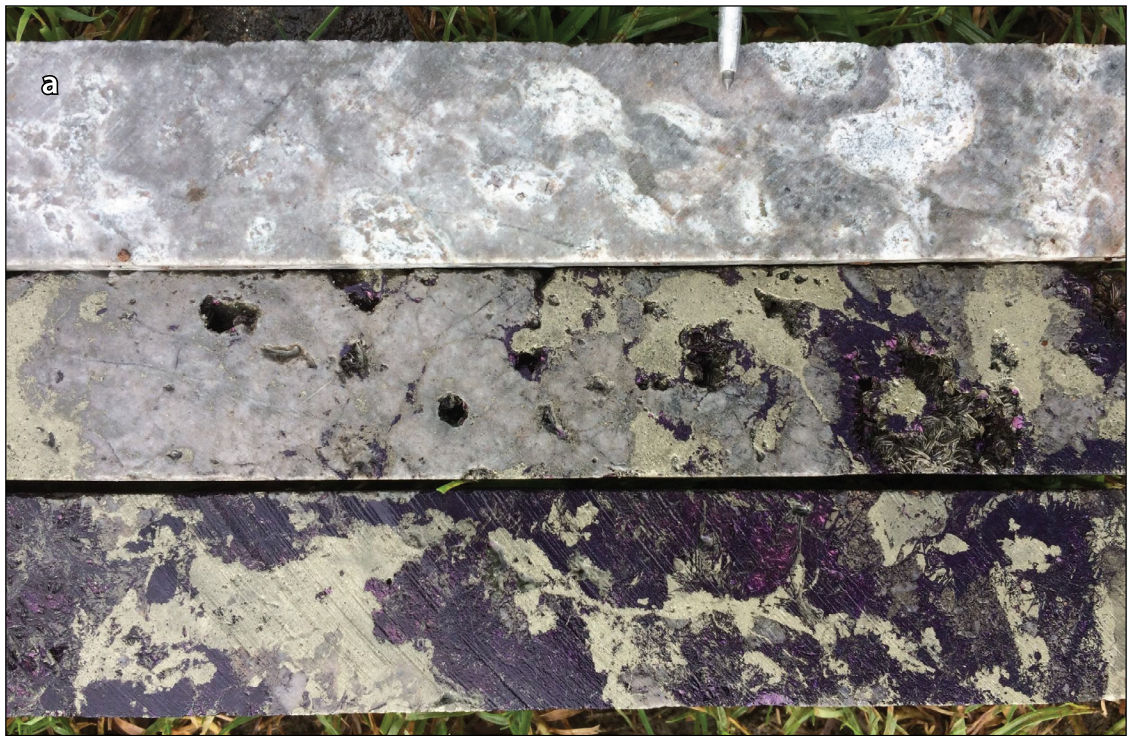

Fig 12. Photographs of typical mineralization in core a) VHD080, interval 757.5 to 760.3 m (~ –393m RL). Three pieces of core from a 3-m interval showing mineralizing process. Patchy textured quartz-alunite alteration (top) becomes progressively leached of alunite to form large vugs that are filled dominantly with pyrite (center) and then covellite (bottom). 4.6% Cu and 1.35 g/t Au with 23% S (4 m), including 2-m interval of 6.8% Cu and 1.85 g/t Au; patchy quartz-alunite alteration is developed in polymictic breccia b) VHD083R–710.25 m (–255 m RL), pyrite-covellite veins with K-alunite halo in late intermineral porphyry, which cut quartz-pyrophyllite ± alunite alteration. c) VHD089–378 m, native sulfur growing on alunite which fringes covellite in vug. From silicified interval within quartz-alunite alteration zone. d) VHD039–1,022 m, Delicate intergrowth of covellite and native sulfur in a steep vein indicating very sulfur rich fluids and extremely high sulfidation state. 2-m interval grades 0.51% Cu and 0.37 g/t Au. e) VHD045–1,118 m, typical pyrite-covellite vein with several generations of pyrite followed by coarse covellite filling open space. f) VHD042–540 to 542 m, irregular covellite vein within lower part of silicic horizon; 14.7% Cu and 32.4 g/t Au. g) VHD072–359.4 m, covellite ± pyrite intergrown and rimmed by nukundamite in vuggy residual quartz alteration in polymictic breccia. 29% Cu and 0.07 g/t Au with 0.9% As, 1 m.

Fig 12. *(Cont.)*

3. Discrete pyrite-covellite veins and veinlets, typically 5 to 10 cm wide, locally up to 0.5 m wide, have steep angles, particularly near the top of the ore zone just below the silicic horizon (Fig. 12e). A subtype occurs within and adjacent to faults that cut the silicic horizon, with covellite-dominated veins and replacement zones in the silicic horizon (Fig. 12f, g). Gold grades are typically low, with Cu/Au (%:g/t) ratios ≥5:1.

Geochronology

Some preliminary geochronology has been undertaken to further constrain the timing of volcanism and porphyry intrusion, and to constrain the timing of alteration and mineralization. Six rock types were dated by U-Pb zircon methods, five alunite-bearing samples were dated using $^{40}Ar/^{39}Ar$ methods, and four samples of molybdenite were dated using Re-Os methods. The results for age determinations are summarized in Tables 2 to 4 and in Figure 13. Methodology for U-Pb zircon, $^{40}Ar/^{39}Ar$ alunite, and Re-Os molybdenite analyses are described in the Appendix. All ages herein are quoted to a 2σ level of uncertainty.

U-Pb ages

Six samples, one each from the capping andesite and the polymictic breccia, two from upper sedimentary package and two porphyry intrusions (early porphyry and early intermineral porphyry) have had host zircons dated by laser ablation-inductively coupled plasma mass spectrometry (LA-ICPMS) (GEMOC, 2015). Table 2 summarizes the analytical results. The samples contain abundant zircon grains that are morphologically very similar. They are typically clear, colorless, euhedral zircon grains and display sector zonation under cathodoluminescence. Grain size is 40 to 200 μm, with most grains about 100 μm. The morphology of the grains indicates crystallization in a magma chamber, not during eruption or late intrusion; thus, the ages are a maximum for geologic emplacement of the host rocks.

Analyses of zircon grains by LA-ICPMS of the six samples yield very young ages (mostly less than 1 Ma). The grains also typically have low uranium contents (<100 ppm). These two factors mean that the grains contain very little radiogenic lead, leading to limitations in precision. To overcome the problem of low lead concentrations a large spot size (65 μm) was used. The low uranium contents and the young ages prevent the derivation of a concordia age for the six samples. Owing to the very young nature of the zircons, a correction for initial ^{230}Th disequilibrium has been applied using an initial Th/U ratio of 2.63. The initial ratio was determined via whole-rock chemical analysis of the capping andesite, which is not significantly affected by alteration, and then applied to all samples. Calculated ages are weighted mean ages for the entire zircon population that typically spans ~600 ka so the ages are maximum ages as zircons may have crystallized in magma chambers rather than during final magma emplacement. No attempt was made to define a weighted mean age based on the youngest statistically valid single population that might better define the porphyry crystallization age (cf. Buret et al., 2016).

The matrix-dominated polymictic breccia sample returned $^{206}Pb/^{238}U$ ages ranging from 0.1 to 1.5 Ma, with a weighted average of 0.716 ± 0.081 Ma. The Th-corrected $^{206}Pb/^{238}U$ ages

Table 2. Summary of U-Pb Age Determinations from Zircon at Onto

Material dated	Sample location	RL (m)	Sample no.	Total spots	Spots used	^{230}Th disequilibrium correction					
						Age (Ma)	± 2σ	MSWD	Age (Ma)	± 2σ	MSWD
LA ICPMS U-Pb results											
Capping andesite	VDH_048, 172–172.8 m	+345	156901	32	30	0.780	0.063	2.8	0.709	0.062	5.4
Pyroclastic interval in upper sedimentary package	VHD042, 297.7–298.5 m	+200	156902	34	33	0.772	0.087	5.9	0.804	0.074	7.6
Matrix-supported polymictic breccia with weak illite smectite alteration	VHD049, 295.1–295.9 m	+267	156903	32	30	0.716	0.081	4.2	0.730	0.110	10.6
Late intermineral porphyry with epidote-chlorite-rutile alteration	VHD049, 1,157.7–1,160.2 m	–569	156904	24	22	0.657	0.075	2.7	0.645	0.067	6.8
Early porphyry	VHD039, 1,042–1,045.3 m	–565	156905	34	31	0.526	0.077	3.9	0.541	0.069	7.7
Upper sedimentary package with vuggy residual quartz alteration	VHD050, 157.20–158.5 m	+220	156906	37	35	0.850	0.046	1.8	0.890	0.054	4.0
SHRIMP U-Pb results											
Capping andesite	VDH_048, 172–172.8 m	+345	156901	24	23	0.745	0.035	1.06	0.838	0.039	0.94
Early porphyry	VHD039, 1,042–1,045.3 m	–565	156905	26	24	0.582	0.052	1.2	0.688	0.053	0.83

MSWD = mean square of weighted deviations; RL = relative to sea level for beginning of range if sample is an interval

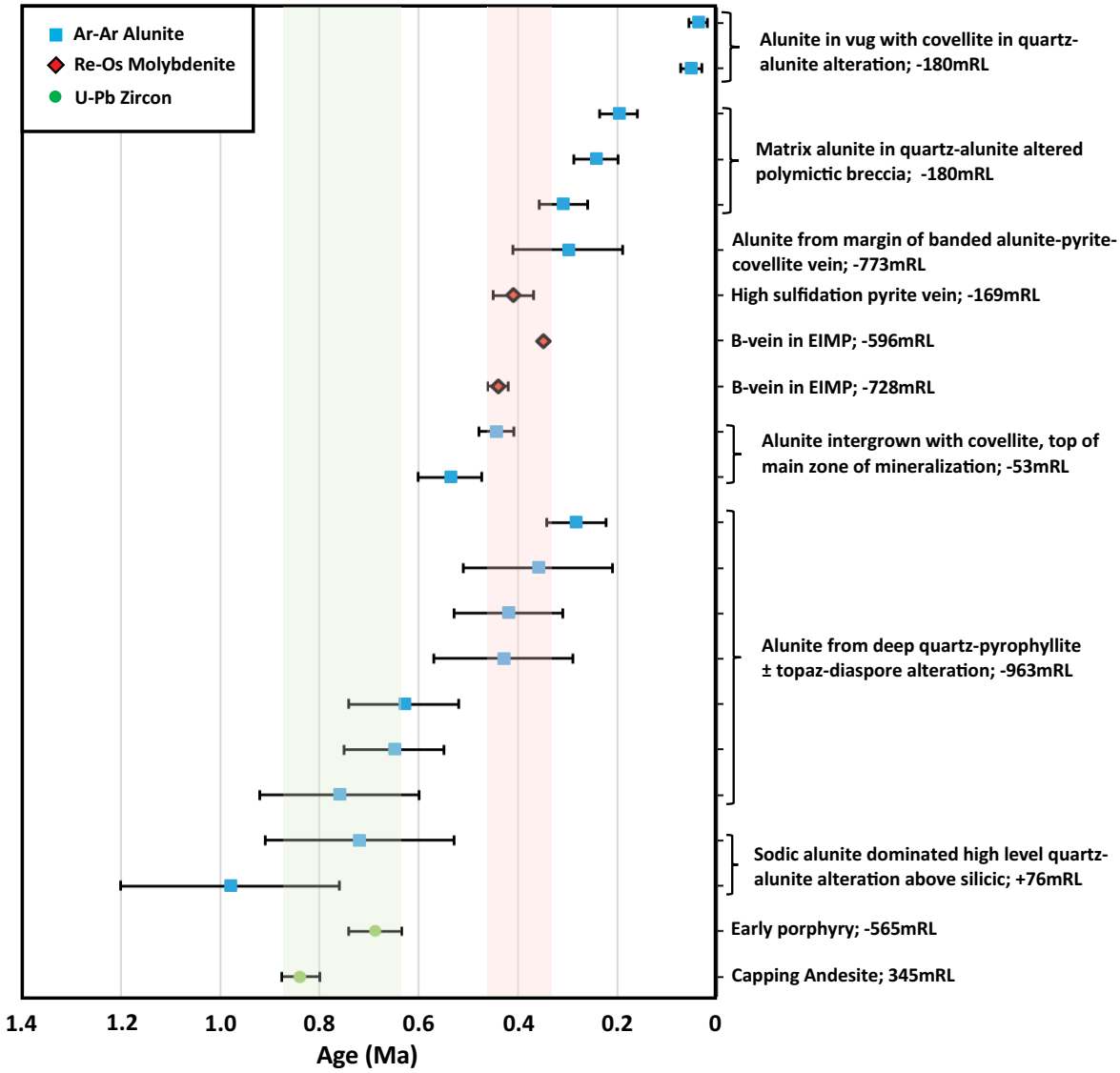

Fig. 13. Summary of geochronology for Onto. Data point error symbols are 2σ. All data are listed in Tables 2, 3, and 4. U-Pb ages are ^{230}Th disequilibrium corrected. Ar-Ar ages are isochron ages. For reference, the pale green color bar shows U-Pb zircon age range for host rocks and the pale red one the range of Re-Os age dates on molybdenite. Abbreviations: EIMP = early intermineral porphyry, RL = elevation relative to sea level.

have a weighted mean of 0.730 ± 0.110 Ma, which is interpreted as the time of igneous zircon crystallization. Two samples from the upper sedimentary package returned ^{206}Pb/^{238}U ages ranging from 0.2 to 1.2 Ma, with a weighted average of 0.772 ± 0.087 Ma, and ^{206}Pb/^{238}U ages ranging from 0.4 to 1.1 Ma, with a weighted average of 0.850 ± 0.046 Ma. The Th-corrected ^{206}Pb/^{238}U ages have a weighted mean of 0.804 ± 0.074 and 0.890 ± 0.054 Ma. A sample of the capping andesite returned ^{206}Pb/^{238}U ages ranging from 0.4 to 1.2 Ma, with a weighted average of 0.780 ± 0.063 Ma. The Th-corrected ^{206}Pb/^{238}U ages have a weighted mean of 0.709 ± 0.062 Ma.

The early porphyry sample returned ^{206}Pb/^{238}U ages ranging from 0.2 to 1.5 Ma, with a weighted average of 0.536 ± 0.077 Ma. The Th-corrected ^{206}Pb/^{238}U ages have a weighted mean of 0.541 ± 0.069 Ma. The late intermineral porphyry sample returned ^{206}Pb/^{238}U ages ranging from 0.4 to 1.4 Ma, with a weighted average of 0.657 ± 0.075 Ma. The Th-corrected ^{206}Pb/^{238}U ages have a weighted mean of 0.645 ± 0.067 Ma.

Owing to the very young nature of the zircons, additional analysis of the capping andesite and early porphyry samples was undertaken using sensitive high-resolution ion microprobe (SHRIMP) by Arise Geoscience Pty Ltd (Table 2). Also owing to the young age and to the low U, the areas analyzed have elevated total ^{207}Pb/^{206}Pb ratios and so the calibrated, uncorrected ratios plot above the Tera-Wasserburg concordia. For the capping andesite, the probability density plot of radiogenic ^{206}Pb/^{238}U ages shows a simple bell-shaped distribution, perhaps with a slight tail on the younger age side. A weighted mean for the 24 analyses gives a ^{206}Pb/^{238}U age of 0.745 ± 0.041 Ma. The Th-corrected ^{206}Pb/^{238}U ages have a weighted mean for the 24 analyses of 0.838 ± 0.039 Ma,

Table 3. Summary of $^{40}Ar/^{39}Ar$ Age Determinations from Alunite at Onto

Sample	Sample location	RL (m)	Material dated	Sample	Plateau age (Ma)	± 2σ	Statistical density plot age (Ma)	± 2σ
Alunite (1479) intergrown with covellite-pyrite in vugs within a small mineralized silicified vuggy quartz zone from 644.5–653 m within quartz-alunite alteration in polymictic breccia; 2-m interval grades 2.87% Cu, 1.17 g/t Au and 646 ppm As	VHD078, 651 m	–180	Alunite crystals and clusters of crystals from vugs lined with alunite and covellite, suggesting the coprecipitation of these minerals; separated into two samples (9628 and 9629).	9628-01	0.041	0.035	0.056	0.021
				9628-02	0.064	0.029		
				9629-01	0.032	0.041	0.038	0.031
				9629-02	0.053	0.066		
			Three microdrill samples (9631, 9632 and 9634) from same samples above	9631-01	0.327	0.026	0.313	0.028
				9631-02	0.248	0.056		
				9632-01	0.250	0.120	0.251	0.039
				9632-02	0.253	0.043		
				9634-01	0.420	0.170	0.420	0.210
				9634-02	0.320	0.041		
Symmetrical vein with outer alunite, inner pyrite ± enargite with central covellite cutting B veins in EIMP from within quartz-alunite-pyrophyllite alteration	VHD058, 1,226.5 m	–773	White alunite from a vein containing an outer layer of alunite, an intermediate layer of pyrite, and a central layer of covellite	9635-01	0.112	0.061	0.143	0.047
				9635-02	0.191	0.070		
			Gray alunite that forms the base of the vein sampled in 9635 above.	9637-01	0.190	0.046	0.212	0.040
				9637-02	0.251	0.058		
Coarse pinkish K-alunite (1477) intergrown with covellite in moderate silicification in base of silicic with 1.5% Cu, 0.22 g/t Au and 550 ppm As; i.e., very top of Main zone of covellite-pyrite mineralization in quartz-alunite–altered LIMP	VHD076, 598.1 m	–53	Gray alunite from the matrix of quartz-alunite alteration from two microdrills	9638-01	0.600	0.090	0.560	0.084
				9638-02	0.513	0.090		
			Pink alunite from end of one of microdrills; crushed and made into two samples	9639-01	0.481	0.039	0.466	0.036
				9639-02	0.486	0.053		
Na-alunite (1490) in top of quartz-alunite alteration in polymictic breccia above silicic alteration horizon; low Cu (187 ppm), Au (0.02 g/t), and As (60 ppm) with 10% S	VHD075, 365 m	+76	Three microdrill cores retrieved; the end of microdrill core1 was crushed and grains from matrix separated into two samples	9640-01	0.980	0.021	1.010	0.200
				9640-02	1.260	0.740		
			Second microdrill yielded grains of matrix alunite separated into two samples	9641-01	1.060	0.320	1.190	0.260
				9641-02	1.240	0.300		
Alunite (1481) with topaz in quartz-alunite-pyrophyllite-diaspore alteration in LIMP; 957 ppm Cu, 0.15 g/t Au, 342 ppm Mo with 11.9% S	VHD079, 1,430 m	–963	The end of microdrill core 1 was crushed and grains of alunite-diaspore from the yellow matrix were placed in two samples	9642-01	0.359	0.055	0.349	0.056
				9642-02	0.800	0.150	0.800	0.150
			Alunite from the gray matrix of the microcore 1 sample	9643-01	0.802	0.085	0.811	0.099
				9643-02	0.480	0.130	0.520	0.170
			Grains of alunite from the yellow matrix of microcore 2 sample formed two samples	9644-01	0.598	0.080	0.670	0.210
				9644-02	0.450	0.210	0.940	0.350
					1.170	0.180		
			Grains of alunite-diaspore from the gray matrix of the microcore 2 were sampled and split into two samples	9645-01	0.760	0.110	0.750	0.140
				9645-02	0.580	0.160	0.580	0.160

Table 3. *(Cont.)*

Sample	Isochron age (Ma)	± 2σ	$^{40}Ar/^{39}Ar$ ratio of intercept	± 2σ	Central age in probability density plot (Ma)	Isochron age (Ma)	Comments
Alunite (1479) intergrown with covellite-pyrite in vugs within a small mineralized silicified vuggy quartz zone from 644.5–653 m within quartz-alunite alteration in polymictic breccia; 2-m interval grades 2.87% Cu, 1.17 g/t Au and 646 ppm As	0.052	0.021	303.5	6.9	0.050 ± 0.017	0.047 ± 0.012	
	0.038	0.018	301.0	17.0			
	0.318	0.049	299.0	14.0	0.301 ± 0.023	0.248 ± 0.024	9631 isochron age compatible with central age, but probably mixed population with older (~ 0.5 Ma) and younger (~0.1 Ma) alunites
	0.244	0.044	301.6	4.7			
	0.300	0.110	308.4	5.8			The low precision of the results for 9634, which results from the low amounts of radiogenic $^{40}Ar^{*}$, suggests that the grains may be composed of natro-alunite, with a lower K content that the alunite sampled in 9631 and 9632
Symmetrical vein with outer alunite, inner pyrite ± enargite with central covellite cutting B veins in EIMP from within quartz-alunite-pyrophyllite alteration	0.025	0.010	303.3	6.2			The isochron age of 0.025 ± 0.010 Ma is much younger than the plateau and central ages, suggesting mixed generations of alunite in the grains sampled for geochronology; the geochronological results are considered unreliable
	0.198	0.038	303.2	3.8			
Coarse pinkish K-alunite (1477) intergrown with covellite in moderate silicification in base of silicic with 1.5% Cu, 0.22 g/t Au and 550 ppm As; i.e., very top of Main zone of covellite-pyrite mineralization in quartz-alunite–altered LIMP	0.537	0.064	303.6	3.2			
	0.444	0.035	306.9	3.6			Older (~0.53 Ma) and younger (~0.3 Ma) alunite crystals probably exist within the sample
Na-alunite (1490) in top of quartz-alunite alteration in polymictic breccia above silicic alteration horizon; low Cu (187 ppm), Au (0.02 g/t), and As (60 ppm) with 10% S	0.720	0.190	310.5	4.3			Evidence for excess argon suggests that 0.720 ± 0.19 Ma is the most probable age of the alunite matrix in this sample
	0.980	0.220	306.9	2.9			Evidence for excess argon suggests that 0.98 ± 0.22 Ma is the most probable age of the alunite matrix in this sample
Alunite (1481) with topaz in quartz-alunite-pyrophyllite-diaspore alteration in LIMP; 957 ppm Cu, 0.15 g/t Au, 342 ppm Mo with 11.9% S	0.284	0.060	314.3	5.3			Two distinct ages in one sample; the geochronological results suggest a sample composed of various generations of alunites of quite distinct ages, ranging from ~0.8 to 0.3 Ma
	0.760	0.160	315.0	5.7			
	0.650	0.100	311.9	4.1			The two different ages reveal that the sample contains multiple generations of alunites formed at distinct times; the most reliable results for this sample are the isochron ages
	0.430	0.140	305.0	7.1			
	0.420	0.110	321.0	5.9			The grains are composed of distinct generations of alunites. The saddle-shape spectra for 9944-02 suggests the presence of excess 40-argon and the geochronological results are considered unreliable
	1.040	0.200	309.6	6.3			
	0.630	0.110	313.1	4.4			Initial $^{40}Ar/^{36}Ar$ values suggest some excess 40-argon; the results are consistent with the presence of multiple generations of alunites
	0.360	0.150	313.7	4.8			

EIMP = early intermineral porphyry, LIMP = later intermineral porphyry, RL = elevation relative to sea level

Table 4. Summary of Re-Os Age Determinations from Molybdenite at Onto

Material dated	Sample location	RL (m)	Sample	Re (ppm)	± 2σ	^{187}Re (ppm)	± 2σ	^{187}Os (ppb)	± 2σ	Model age (Ma)	± 2σ
MoS_2 in B veins in phyllic-altered early intermineral porphyry	VHD054, 1,324.05–1,330 m	–728	156909	93	0.2	58.7	0.1	0.43	0.02	0.44	0.02
MoS_2 in B-veins in phyllic-chloritic altered early intermineral eorphyry	VHD049, 1,186–1,190.9 m	–596	156908a	7,724	19	4,854.60	11	28.4	0.05	0.35	0.0011
High-sulfidation–style mineralization in banded siliceous pyrite-molybdenite vein cutting quartz-pyrophyllite ± diaspore-alunite alteration in polymictic breccia; within Mo-rich zone (avg = 297 ppm Mo, high of 1,570 ppm Mo) from 506 m (base of silicic) to 634 m downhole	VHD078, 622.2 m	–151	622.2	120.39	8.07	75.67	5.07	0.51	0.03	0.41	0.04
High-sulfidation–style mineralization in banded, crustiform-textured pyrite-alunite-molybdenite vein within quartz-alunite alteration in polymictic breccia; same Mo-rich interval as sample above	VHD078, 590 m	–119	590	7.2	0.02	4.55	0.01	0.03	0.02	0.36	0.27

RL = elevation relative to sea level

which is interpreted as the time of igneous zircon crystallization. For the early porphyry, a weighted mean for 24 analyses (two excluded) gives a $^{206}Pb/^{238}U$ age of 0.582 ± 0.052 Ma. The Th-corrected $^{206}Pb/^{238}U$ ages have a weighted mean for the preferred 24 analyses of 0.688 ± 0.053 Ma. Additional information is provided in the Appendix. SHRIMP data are thought to be more precise and reliable than LA-ICPMS analyses, so these two Th-corrected age dates are the preferred ages plotted in Figure 13.

$^{40}Ar/^{39}Ar$ ages

Five samples of core were submitted for $^{40}Ar/^{39}Ar$ analysis of alunite to the University of Queensland AGES Lab. The samples covered the key advanced argillic alteration assemblages and a total of 15 subsamples were analyzed, each with two individual aliquots. $^{40}Ar/^{39}Ar$ dating methods and analytical details are contained in the Appendix. Table 3 summarizes the analytical results and the following comments are summarized from Vasconcelos and Thiede (2018).

The results show a history of alunite crystallization from very early in the development of Onto to recent times. A number of the samples are composed of several generations of alunites and these generations are identifiable in the results obtained for the subsamples as well as in some cases from probability density plots appearing to contain mixed populations for individual subsamples.

Samples of alunite associated with topaz and diaspore from high-temperature advanced argillic alteration near the base of current drilling 962 m bsl in the late intermineral porphyry returned geochronological results that suggest samples composed of various generations of alunites of quite distinct ages, ranging from ~0.8 to 0.3 Ma. The most reliable isochron ages are as follows: 0.76 ± 0.16, 0.65 ± 0.10, 0.63 ± 0.11, 0.43 ± 0.14, 0.42 ± 0.11, 0.36 ± 0.15, and 0.284 ± 0.060 Ma.

Samples of polymictic breccia with sodic alunite alteration from above the silicic alteration horizon toward the Wadubura end of the system (77 m asl) returned most probable ages of 0.98 ± 0.22 and 0.72 ± 0.19 Ma. Two samples of alunite in strong mineralization at the top of the main zone of mineralization at Onto record alunite crystallization from 0.54 to 0.24 Ma. Isochron ages (each compatible with central ages from probability density plots) are as follows: 0.537 ± 0.064 and 0.444 ± 0.035 Ma from the sample 53 m bsl, and 0.318 ± 0.049, 0.30 ± 0.11, and 0.244 ± 0.044 Ma from the sample 180 m bsl (Fig. 13; Table 3).

In two samples we attempted to age-date alunite intimately associated with covellite. In the first one, white alunite was analyzed from a late banded vein surrounding pyrite, and a central layer of covellite. The probability density plot for all results defines a very broad population of apparent ages with a most probable age peak at 0.1614 Ma and a central age of 0.143 ± 0.047 Ma. The probability density plot appears to contain mixed populations, where some of the alunite is ~50 ka and some may be as old as 200 ka. The isochron age is 0.025 ± 0.01 Ma but this age is considered unreliable as it is much younger than the statistical density plot age. A sample of gray alunite that forms the base of the same late vein described above returned an isochron age of 0.198 ± 0.038 Ma compatible with the central age of 0.212 ± 0.040 Ma from the probability density plot. In the second sample, two subsamples of

alunite from vugs lined with alunite and covellite, suggesting the coprecipitation of these minerals, were analyzed.

In one subsample the isochron age of 0.052 ± 0.016 Ma is compatible with the central age of 0.056 ± 0.021 Ma from the probability density plot and it is the best estimate for the age of the vug-filling alunite. In the second subsample, the isochron age of 0.038 ± 0.018 Ma is compatible with the central age of 0.038 ± 0.031 Ma from the probability density plot and is within error from the age of the first sample. Treated as one sample, the ages for these alunites, intergrown with covellite in vugs, are 0.050 ± 0.017 (probability density plot) to 0.047 ± 0.012 Ma (isochron age).

Re-Os ages

Limited dating of the mineralization has been completed thus far with a total of four samples submitted to the John de Laeter Centre for Isotope Research, Department of Imaging & Applied Physics, Curtin University (Tessalina, 2015, 2017). Analytical methods are provided in the Appendix.

A sample of molybdenite from a B vein in phyllic-altered interval of early intermineral porphyry from VHD054 at 1,325 m returned a double spike Re-Os model age of 0.44 ± 0.02 Ma. A similar sample of phyllic-altered intermineral porphyry from VHD049 at 1,186 m at the margin of the advanced argillic alteration albeit with much higher Re content (Table 4) gave an age of 0.35 ± 0.0011 Ma.

Two samples of molybdenite from high-sulfidation–style banded pyrite-alunite-quartz molybdenite veins from VHD078 at 590 and 622 m yielded ages of 0.36 ± 0.27 and 0.41 ± 0.04 Ma. Molybdenite from the sample at 590 m has significantly lower Re and Os contents and hence high age uncertainty. This age date is not plotted in Figure 13.

Based on the current dating for four samples, the timing of the molybdenum associated with porphyry-related B vein-hosted mineralization and the high-sulfidation style are essentially the same, between 0.44 and 0.35 Ma (Fig. 13).

Fluid Inclusions

A preliminary examination of fluid inclusions at Onto indicates that there are numerous coexisting vapor-rich and NaCl-saturated fluid inclusions, consistent with a low pressure (and shallow depth) of formation. There are also abundant saline melt inclusions, indicating anomalously hot but low-pressure conditions (Fournier, 1999; Muntean and Einaudi, 2000, 2001; Audétat et al., 2008). Preliminary microthermometry of high temperature coexisting NaCl-saturated and vapor-rich fluid inclusions from a sample from 560 m bsl in A vein quartz indicates a minimum depth of 2 km, i.e., paleosurface ~1,440 m asl (Reynolds, pers. commun., 2019). This is consistent with the geologic reconstruction of an original volcanic edifice at ~1,300 m elevation, based on topographic reconstruction from the youngest lava dip slopes near Onto.

Discussion

Age and origin of host rocks

The andesitic sequence in the Hu'u project may have started to develop as far back as 5.2 Ma but most ages for detrital zircons fall between 2.7 and 0.7 Ma. In the Onto area the main component of the volcanosedimentary package is a polymictic breccia that is typically unsorted and unbedded over vertical intervals of at least 1 km surrounded by an earlier sequence of mainly andesite flows. The upper portions of the breccia comprise a clast-supported polymictic breccia with very variable clasts and grades up into a well-bedded sequence of siltstones and interbedded pyroclastic and volcaniclastic rocks. This transition from sediments to vaguely bedded but highly variable breccia to poorly sorted massive breccias at depth, together with juvenile fragments in the breccia, are typical features of diatreme vent complexes formed during phreatomagmatic eruptions (White and Ross, 2011; Ross et al., 2017). The bedded sequence, which was deposited in ephemeral lakes in the maar complex, was then capped by hornblende andesite flow domes.

Since the the top of the diatreme complex and the intramaar sediments are still preserved, there was no significant erosion prior to emplacement of the capping andesite flows. We consider the formation of the diatreme, deposition of the intramaar sediments, and then capping by flow domes most likely occurred within a very short timeframe. The Th-corrected SHRIMP U-Pb zircon crystallization age of 0.838 ± 0.039 Ma from the capping andesite is considered the most robust age for the volcanosedimentatry package at Onto and places an upper limit on the emplacement of the capping andesites.

The Th-corrected SHRIMP U-Pb zircon crystallization age of 0.688 ± 0.053 Ma from the early porphyry is considered the most robust age for the porphyry stocks at Onto and places an upper limit on the emplacement of the porphyries into the diatreme breccia. The porphyry intrusions intruded to approximately 50 m bsl and irregular "wormy," high-level A veins in the two earliest phases of the porphyry stocks indicate preservation of the original cupulas of the porphyry stocks. We speculate that the capping andesites may have originally reached a maximum height of 1,200 to 1,300 m asl, based on topographic reconstruction from the youngest lava dip slopes near Onto, indicating the intrusions reached a shallow level, perhaps within 1.3 km of the paleosurface.

Hydrothermal alteration in lithocap

The earliest, hottest, and most widespread advanced argillic alteration type at Onto is quartz-pyrophyllite-diaspore with minor topaz and zunyite. Diaspore with topaz and zunyite tend to become more common deeper than ~600 m bsl, but higher-level remnants of this alteration, evidenced by SWIR-based identification of zunyite, diaspore, and topaz, are occasionally present to approximately sea level in many holes (Fig. 8). Pyrophyllite extends higher, to ~100 m asl, in several cases even higher above quartz-alunite and even quartz-dickite alteration zones to about 300 m asl. The top of the early alteration is marked by quartz-dickite (~200° to <270°C), quartz-kaolinite, and the uppermost illite-smectite (<200°C) alteration. Experimental results by Hemley et al. (1980) indicate pyrophyllite and diaspore should not coexist at temperatures less than 280°C. Hsu (1986) reported zunyite is stable up to 450°C, where it is replaced by topaz at higher temperatures. This alteration is thus interpreted to have formed at temperatures ≥300°C from ascending magmatic vapor after brine-vapor separation in the porphyries.

In the greater part of the Onto deposit area, this early advanced argillic alteration is partially to completely

overprinted by thick quartz-alunite alteration zones typically dominated by K-alunite, especially in the upper parts (Figs. 4b, 8). This alteration extends as consistent roots down through the quartz-pyrophyllite-diaspore, but more commonly only partially replaces the earlier alteration. Quartz-alunite alteration probably formed from ponded acidic fluids generated by condensation of SO_2-rich magmatic vapor containing acidic volatiles (e.g., Watanabe and Hedenquist, 2001). Modeling by Hedenquist and Taran (2013) indicates alunite is stable between ~200° and 300°C and dominates in abundance over aluminosilicate minerals under more oxidized conditions and that pyrophyllite becomes increasingly unstable under higher water/rock ratios. Ar-Ar ages from alunite yield a wide range of dates, from 0.98 ± 0.22 to 0.198 ± 0.038 Ma, with some samples intergrown with covellite in late vugs giving younger ages between 0.052 ± 0.021 and 0.038 ± 0.018 Ma. (Fig. 13).

Numerous clasts of quartz-alunite and vuggy residual quartz as well as mineralized veined-porphyry clasts in the diatreme polymictic breccia indicate some lithocap development and mineralized porphyry emplacement preceded diatreme formation but the exact timing and extent of this event has not been established. The capping andesite in a few drill holes also contains clasts of magnetite-rich rock.

Alunite ages of 0.98 + 0.22 and 0.72 + 0.19 Ma from sodic alunite toward the Wadubura end of the system (77 m asl) overlap with the U-Pb zircon age for the capping andesite, indicating that advanced argillic alteration continued immediately after diatreme formation.

The oldest reliable alunite age of 0.76 ± 0.16 Ma from alunite associated with topaz and diaspore, near the base of current drilling 962 m bsl, in the late intermineral porphyry overlaps with the U-Pb zircon crystallization age from the early porphyry, suggesting almost immediate advanced argillic alteration of the porphyry stocks during or immediately following emplacement and that advanced argillic alteration was potentially occurring over at least 1 km vertical thickness by this time. It follows that if the porphyries intruded into rocks that had already undergone advanced argillic alteration, then the reduced rock buffer probably enhanced early development of the high-sulfidation assemblages in the mineralization.

The silicic alteration zone could represent ponding of cooling vapor condensate below ≤200°C at low pH <1, where only quartz, pyrite, and native sulfur are stable and alunite dissolves (Hedenquist and Taran, 2013), forming vuggy residual quartz. Once vuggy residual quartz had formed it was overprinted by pervasive silicification. At Onto, the persistent nature and subhorizontal attitude suggest formation of the silicic alteration zone beneath a paleowater table, as quartz-saturated water cooled and precipitated quartz in proximity to the water table (Longo, 2000).

At Onto, the advanced argillic alteration zonation is intact and in the immediate Onto area there is minimal indication at surface of the quartz-alunite-pyrophyllite alteration that hosts mineralization, except in the northwestern Wadubura area where the lithocap partially crops out. In this area quartz-dickite and vuggy quartz alteration is overprinted by a porous white, powdery, steam-heated assemblage composed of cristobalite, kaolinite, and sulfur ± sodic alunite. This surface alteration is continuous with but probably overprints the upper porous, vuggy quartz horizon (Fig. 4b). In the northwestern area it lies directly on top of the lower horizon as the two horizons merge (Fig 4b). The upper porous vuggy quartz horizon is thus confidently interpreted as a paleogroundwater table, notwithstanding the fact that the overlying andesite porphyry is only weakly smectite altered in many places rather than being converted to a white, powdery, steam-heated assemblage composed of cristobalite ± alunite.

Pyrophyllite is also found in the high-level quartz-dickite alteration as well as occurring in the deep quartz-pyrophyllite-diaspore alteration. Although pyrophyllite is thought to form in a temperature range between 280° and 360°C (Watanabe and Hedenquist, 2001), it can form at a lower temperature if the fluid phase is supersaturated with respect to silica and has been interpreted to form at temperatures as low as ~200°C (Knight, 1977; Reyes, 1990) and overlap the stability field for dickite.

Finally, a persistent feature of the alteration zonation at Onto is the occurrence of illite-smectite alteration zones consistently within and below the quartz-dickite alteration, often separating the latter from the underlying quartz-alunite alteration. This relationship is observed in the majority of holes, suggesting the acidic fluids causing quartz-dickite ± pyrophyllite alteration in the higher part of the system moved laterally in discrete flow zones, in contrast to the underlying quartz-alunite and vuggy residual quartz alteration that is pervasive and intense, resulting from a broad vapor plume (Henley and McNabb,1978).

Onto deposit model

The main phase of copper and gold introduction is thought to have accompanied emplacement of the first two porphyry phases and is associated with an intense, high-temperature A-B vein quartz veinlet stockwork developed at the top of these intrusions over a ~350-m vertical interval mainly between 100 and 500 m bsl. Where the quartz veinlet stockwork is occasionally preserved at the sides and, in a few cases, below the advanced argillic alteration package, the stockwork contains magnetite with chalcopyrite ± bornite and pyrite associated with potassic (magnetite, secondary biotite) and chlorite-sericite alteration. In rare cases, small 5- to 50-μm chalcopyrite-bornite and more rarely bornite-chalcocite inclusions are observed in pyrite associated with covellite adjacent to early A quartz veinlets (Fig. 11c) and in quartz; these are interpreted as relicts of the earlier low- to intermediate-sulfide assemblage encapsulated in pyrite and quartz during the high-sulfidation overprint. Porphyry-style mineralization related to potassic alteration has average grades of 0.8% Cu and 0.76 g/t Au in the early porphyry, 0.58% Cu and 0.25 g/t Au in the early intermineral porphyry and 0.41% Cu and 0.13 g/t Au in the late intermineral porphyry with arsenic values in the three porphyry phases of ~120 ppm; in the most pristine material arsenic values are <45 ppm with sulfur values ~4.7%.

In the area drilled at Onto, within a tabular zone measuring at least 1.5 × 1 km with a vertical thickness of ≥1 km, the diatreme breccia, all porphyry intrusions, and to a lesser extent the surrounding early andesite sequence have been overprinted by intense advanced argillic alteration, predominantly quartz-alunite and quartz-pyrophyllite ± diaspore alteration (Fig. 8), and high-sulfidation–style covellite-pyrite mineralization totally predominates.

Despite the intense high-sulfidation overprint, with addition of ~300 ppm arsenic, sulfur (avg ~11%), and other metals to the mineralized system, the copper and gold remain remarkably close the porphyry stocks with 60% of the current copper-gold resource at 0.3% Cu cutoff within the stocks, with the remainder hosted in pre-mineral diatreme, largely above the porphyry intrusion complex. Several holes on the margin of Onto without porphyry intrusions, despite thick and intense quartz-alunite-pyrophyllite alteration, do not contain significant Cu-Au mineralization.

Average copper and gold grades in the three main porphyry phases within the 0.3% Cu envelope, predominantly in quartz-alunite-pyrophyllite ± diaspore alteration, are ~1.2% Cu and 0.7 g/t Au, 0.9% Cu, and 0.4 g/t Au, and 0.6% Cu and 0.3 g/t Au in the early and late intermineral porphyries, respectively. The grades and copper-gold ratios, at least in the two earliest porphyry phases, are quite similar to those preserved in potassically altered porphyry-style mineralization, indicating the quartz-alunite-pyrophyllite alteration and the high-sulfidation overprint do not radically change copper and gold distribution.

Metal-bearing fluids at Onto are postulated to have rapidly evolved to a very high sulfidation state on cooling due to the lack of a rock buffer in the thick, advanced argillic alteration (Einaudi et al., 2003), resulting in deposition of covellite-pyrite and widespread native sulfur. Covellite is intergrown with pyrophyllite, alunite, dickite, and native sulfur, and it occurs as coarse-bladed crystals in pyrophyllite and diaspore aggregates (Fig. 11a, b) and along with pyrite as fine inclusions in zunyite; all indicating covellite deposition must have spanned a wide temperature range, perhaps from ≥300° to ~100°C as it is intergrown with pyrophyllite, alunite, dickite, and native sulfur (Reyes, 1990; Watanabe and Hedenquist, 2001).

Covellite totally replaced the original high-temperature intermediate copper sulfide assemblages within and adjacent to A-B quartz veinlets. Then, with pyrite, it filled the open space generated during the advanced argillic alteration with some of the higher-grade material occurring within local zones of vuggy residual quartz within the quartz-alunite alteration and interstitial to relict quartz veinlet stockworks where all but the quartz vein material was leached away (Figs. 7e, 10b).

As well as seemingly being intergrown with high-temperature minerals, covellite and pyrite are also found in delicate intergrowths in open filling with alunite, dickite, and native sulfur (Fig. 12c, d), and pyrite-covellite veins sometimes have alunite alteration halos. These features clearly indicate that covellite-pyrite precipitation in both open-space fillings and in veins is closely related to on-going advanced argillic alteration by low-temperature, low-pH fluids, rather than there being a time gap between creating porosity and permeability during advanced argillic alteration and introducing a different fluid at a later stage, as has been suggested for some other epithermal deposits such as Lepanto (Hedenquist et al., 1998).

At this time, the mechanism by which advanced argillic alteration and high-sulfidation–style mineralization overlaps with porphyry-related mineralization at Onto is not clear. The porphyry- and high-sulfidation styles of mineralization overlap spatially and, based on Re-Os, date temporally at ~0.4 Ma. Based on the maximum height of the original volcanic edifice overlying the Onto area and the current land surface, less than 600 m has been removed in the ~400,000 years, implying relatively low degradation rates and there does not appear to be evidence for a large mass-wasting event that would have produced telescoping (Sillitoe, 1994). The zoned advanced argillic alteration appears to have only ever extended ~250 to 300 m above the apices of the porphyry stocks and only locally reached the surface in the deposit area, but alteration extends down to vertical depths that locally exceed 1,200 m within the deposit footprint.

Deposit analogies and implications for exploration

The degree to which covellite dominates with >90% of copper deportment is unusual as most high-sulfidation Cu-Au deposits are enargite-dominated and composed of massive sulfide replacements and breccias (Sillitoe, 1983, 1999). Covellite dominance at Onto has some similarities to Bor deposits and the recently discovered Cukaru Peki deposit in Serbia, where small, high-sulfidation massive sulfide zones that overlie the porphyry mineralization are covellite dominated (Herrington et al., 1998; Pittuck, 2014). Analogies can also be drawn with the deeper unoxidized portions of Cerro Yanacocha Complex gold deposits where below the Yanacocha Sur pit deeper hypogene sulfide mineralization is dominated by enargite and then covellite associated with quartz-pyrophyllite alteration before grading downward to chalcopyrite-dominant Cu-Fe sulfides in the Yanacocha dacite porphyry (Longo et al., 2010; Teal and Benavides, 2010; Pilco, 2011). The Zijinshan high-sulfidation epithermal deposit in mainland China (Chen et al., 2019) also contains appreciable covellite with pyrite but in this case accompanied by digenite and minor enargite, chalcocite, and bornite in veins and breccias.

Covellite dominance may reflect As-deficient fluids, perhaps in a very proximal environment close to the porphyry source, or in the oxidized, high SO_2-rich fluids, arsenic was flushed to the margins of the system and perhaps enargite-dominated mineralization is yet to be discovered outboard of Onto deposit as currently defined; enargite is certainly more prevalent in the drill holes marginal to main zone of mineralization. It is interesting to note that no significant gold-only mineralization has been located to date at Onto within the 0.3% copper envelope, rather the mineralization is copper-dominated with an overall Cu/Au ratio (%:g/t) of ~2:1.

The high copper-gold grades, the large size, and good grade continuity at Onto are thought to be related to a number of factors. Firstly, high copper and gold tenors could be attributed to preexisting high-grade copper-gold mineralization in the most intense A- and B-type quartz stockworks in the porphyry stocks, as typical of mineralization in the top of the quartz stockwork shell in many porphyry systems. Secondly, the advanced argillic overprint was particularly intense and largely contained within the diatreme breccia and intrusives, perhaps as cooling magmatic vapor ponded below the sediments and capping and andesite, and the impermeable silicic horizon once it formed. This containment of the magmatic volatiles led to the almost total replacement of an original low- to intermediate-sulfidation assemblage of chalcopyrite ± bornite and pyrite by a high-sulfidation assemblage of covellite and pyrite. The SO_2-rich acidic fluids, causing advanced argillic alteration, remobilized and dispersed early copper and, to a lesser extent, gold as disseminations and veins but

also may also have deposited additional copper and gold. This led to originally less well mineralized rocks, such as the late intermineral porphyry, being upgraded and also homogenization of grade as a whole, such that low-grade areas have not been identified within the main copper-gold grade shell at a 0.3% Cu cutoff.

Conclusions

A deep drilling program at Onto in an extensive advanced argillic alteration lithocap within the Hu'u project on eastern Sumbawa Island, Indonesia, has discovered a large covellite-pyrite dominated porphyry/high-sulfidation epithermal deposit, hosted in quartz-alunite-pyrophyllite alteration at ~500 m below surface with little surface expression in the immediate deposit area. Total indicated and inferred resources currently stand at 1.7 Gt at 0.89% Cu and 0.49 g/t Au with contained copper of 15 Mt and 27 Moz of gold. Mineralization is related to a series of small, coalesced, high-level porphyry stocks that top out as small intrusions at about sea level, approximately 600 m below current land surface. The porphyry intrusions expand gradually with depth covering an area of ~1.6 × 0.6 km at 500 m bsl. The porphyries intruded just after 0.688 ± 0.053 Ma into the central portion of a large maar-diatreme vent breccia that formed and was capped by maar sediments and then andesite flows just after 0.838 ± 0.039 Ma. The copper-gold resource (at 0.3% Cu cutoff) is largely contained within the porphyries (60%) with the remainder mostly above the porphyry stocks in the premineral diatreme breccia. A small proportion of the current source (<8%) occurs as typical porphyry-style disseminated chalcopyrite-bornite-pyrite mineralization in potassic alteration associated with wide A and B quartz veinlet stockwork shells at the margins of the advanced argillic alteration, but in general the porphyry stocks are intensely overprinted by quartz-alunite and quartz-pyrophyllite ± diaspore alteration (90% of current resource) down to more than 1 km depth. With little rock buffering capacity, metal-bearing fluids at Onto are postulated to have rapidly evolved to a very high sulfidation state on cooling in the thick advanced argillic alteration, resulting in deposition of covellite-pyrite and widespread native sulfur. This assemblage totally replaced earlier sulfides, infilled vugs and open space generated during the intense advanced argillic alteration, and formed late pyrite-covellite and covellite-only veins. Unlike some high-sulfidation gold-copper deposits, where there may be a considerable time gap between "ground preparation" by dissolution by the highly acidic fluids and deposition of sulfides in the open space generated, at Onto pyrite and covellite are intergrown with a variety of minerals forming during advanced argillic alteration. Covellite is intergrown primarily with alunite and native sulfur, but also several higher-temperature aluminosilicates, suggesting a wide range of temperature for covellite precipitation, including down to very low temperatures, where late fluids supersaturated in SO_2 contained enough sulfur to precipitate native sulfur after Cu and Fe sulfides were deposited.

The advanced argillic-altered system has a subhorizontal attitude and is largely uneroded, with a vertical zonation from illite-smectite, though quartz-dickite-kaolinite to quartz-alunite to quartz-pyrophyllite ± diaspore at depth and only ever extended ~250 to 300 m above the apices of the porphyry. The mineralized envelope is capped by persistent 100- to 300-m-thick silicic horizon that effectively restricted fluids, and unless heavily fractured contains minimal mineralization (<2% of resource). The only surface geochemical expression of the blind Onto deposit is some weak copper dispersion related to late phreatic breccia and faults that pierce through the silicic horizon.

The Onto mineralization is exceptionally young and the system formed rapidly in the middle Pleistocene between ~0.7 Ma and present, with copper-gold mineralization probably spanning a period of ~100 ky, between 0.44 and 0.35 Ma, based on the Re-Os model ages for molybdenite followed by some remobilization and perhaps additional copper and gold added to the system to as recently as ~38 ky. This makes Onto the youngest giant to supergiant hybrid copper-gold porphyry/high-sulfidation epithermal system discovered.

More research is required to determine if the fluid that caused potassic alteration and porphyry-style mineralization evolved, through interaction with extensive advanced argillically altered rocks, to fluids that deposited the very high sulfidation assemblage of covellite and pyrite, or whether a separate, lower-temperature fluid was involved. Either way, Re-Os dating of molybdenum associated with both the porphyry-related B vein-hosted mineralization and the high-sulfidation–style pyrite veins suggest both formed within a very short period between 0.44 and 0.35 Ma. More work is also required to determine how much of the copper was deposited directly as covellite and how much covellite forms from sulfidation of bornite-chalcopyrite, and along the same lines, whether copper and gold were continuously added to the system or just remobilized and dispersed away from existing mineralization centered on the two earliest porphyries.

Acknowledgments

This paper is dedicated to the memory of Peter Winterburn, Vale's chief geochemist who was killed during an attempted robbery in Valparaiso, Chile, on June 21, 2019. Peter provided crucial input to this and many other Vale projects worldwide, and he is sorely missed.

Discoveries are made possible by large dedicated teams and Onto is no exception. The local Indonesia-based team was given considerable latitude and flexibility in executing the program and empowered to drill a series of deep holes through a barren lithocap by the director of exploration, Fabio Masotti.

Mike Rennison was the regional manager for business development and project generation Australasia and David Burt the country manager at the time of discovery, while Lawrie Jorgensen was country manager at the time the Contract of Work was joint-ventured and was involved at an early stage, as was Inco's and Vale's long-standing country manager Beni Wahju, since deceased. Mike Hillier supervised all assaying and provided QAQC for geochemistry, while Richard Hague was responsible for resource estimates.

A large team of Indonesian geologists and support staff were an integral part of the discovery and subsequent delineation—in particular, Nur Tyas Mudadi, Nurhadi Wibowo, Kristison Situmorang, Za Munarfan Putra, Douglas Simaremare, Fahmi Setiawan, Gina Pariana, and Rachmat Pratiwinda. Dick Sillitoe provided significant insights in logging core during a visit in 2012 and again in November 2015.

Graham Teale provided excellent petrographic descriptions, Mark Fanning completed the SHRIMP analyses, and Jim Reynolds is thanked for preliminary fluid inclusion petrography and microthermometry along with discussion of the results. Rod Jones is acknowledged for his long-standing belief that the Hu'u project had the potential to contain a significant copper deposit. Tony Longo is thanked for a detailed and thoughtful review that greatly improved the manuscript. David Cooke is thanked for his review and also Jeff Hedenquist for reviewing and editing an earlier version of this manuscript.

REFERENCES

Arribas, A., Jr., Hedenquist, J.W., Itaya, T., Okada, T., Concepción, R.A., and Garcia J.S., Jr., 1995, Contemporaneous formation of adjacent porphyry and epithermal Cu-Au deposits over 300 ka in northern Luzon, Philippines: Geology, v. 23, p. 337–340.

Audétat, A., Pettke, T., Heinrich, C.A., Bodnar, R.J., 2008, The composition of magmatic hydrothermal fluids in barren versus mineralized intrusions: Economic Geology, v. 103, p. 877–908.

Buret, Y., von Quadt, A., Heinrich, C., Selby, D., Wällea, M., and Peytchevaa, I., 2016, From a long-lived upper-crustal magma chamber to rapid porphyry copper emplacement: Reading the geochemistry of zircon crystals at Bajo de la Alumbrera (NW Argentina): Earth and Planetary Science Letters, v. 450, p. 120–131.

Cerpa, L.M., Bissig, T., Kyser, K., McEwan, C., Macassi, A., and Rios, H.W., 2013, Lithologic controls on mineralization at the Lagunas Norte high sulfidation epithermal gold deposit, northern Peru: Mineralium Deposita, v. 48, p. 653–673.

Chen, J., Cooke, D.R., Piquer, J., Selley, D., Zhang, L., and White, N.C., 2019, Hydrothermal alteration, mineralization, and structural geology of the Zijinshan high-sulfidation Au-Cu Deposit, Fujian Province, southeast China: Economic Geology, v. 114, p. 639–666.

Chouinard, A., Williams-Jones, A.E., Leonardson, R.W., Hodgson, C.J., Silva, P., Téllez, C., Vega, J., and Rojas, F., 2005, Geology and genesis of the multistage high-sulfidation epithermal Pascua Au-Ag-Cu deposit, Chile and Argentina: Economic Geology, v. 100, p. 463–490.

Deditius, A.P., Utsunomiya, S., Renock, D., Ewing, R.C., Ramana, C.V., Becker, U., and Kesler, S.E., 2008, A proposed new type of arsenian pyrite: composition, nanostructure and geological significance: Geochimica et Cosmochimica Acta, v. 72, p. 2919–2933.

Einaudi, M.T., Hedenquist, J.W., and Inan, E.E., 2003, Sulfidation state of fluids in active and extinct hydrothermal systems: transitions from porphyry to epithermal environments: Society of Economic Geologists Special Publication 10, p. 285–314.

Fournier, R.O., 1998, Hydrothermal processes related to movement of fluid from plastic to brittle rock in the magmatic-epithermal environment: Economic Geology, v. 94, p. 1193–1211.

Garwin, S., Hall, R., and Watanabe, Y., 2005, Tectonic setting, geology, and gold and copper mineralization in Cenozoic magmatic arcs of southeast Asia and West Pacific: Economic Geology 100th Anniversary Volume, p. 891–930.

Garwin, S.L., 2002, The geologic setting of intrusion-related hydrothermal systems in the vicinity of Batu Hijau porphyry copper gold deposit, Sumbawa, Indonesia, Society of Economic Geologists, Special Publication 9, p. 333–366.

GEMOC, 2013, U-Pb Dating of zircons from stream concentrates, Hu'u, Indonesia; Samples 137231, 137232, 137233, 137234, 137235 & 137236: Preliminary Report to Vale. June 2013 TerraneChron® Confidential Report, TC-124_Preliminary Report.

——2015, U-Pb Dating of zircons; Samples 156901, 156902, 156903, 156904, 156905 & 156906: Confidential Report TC-154, Internal Vale Report.

Gustafson, L., Vidal, C., Pinto, R. and Noble, D., 2004, Porphyry-epithermal transition, Cajamarca region, northern Perú: Society of Economic Geologists Special Publication 11, p. 279–300.

Harrison, R., Maryono, A., Norris, M., Rohrlach, B., Cooke, D., Thompson, J., Creaser, R., Thiede, D., 2018, Geochronology of the Tumpangpitu porphyry Au-Cu-Mo and high-sulfidation epithermal Au-Ag-Cu deposit: Evidence for pre- and post-mineralization diatremes in the Tujuh Bukit district, southeast Java, Indonesia: Economic Geology, v. 113, p. 163–192.

Hedenquist, J.W., and Taran, Y.A., 2013, Modeling the formation of advanced argillic lithocaps: volcanic vapor condensation above porphyry intrusions: Economic Geology, v. 108, p. 1523–1540.

Hedenquist, J.W., Arribas, A., Jr., and Reynolds, T.J., 1998, Evolution of an intrusion-centered hydrothermal system: Far Southeast-Lepanto porphyry and epithermal Cu-Au deposits, Philippines: Economic Geology, v. 93, p. 373–404.

Heinrich, C.A., 2005, The physical and chemical evolution of low- to medium-salinity magmatic fluids at the porphyry to epithermal transition: A thermodynamic study: Mineralium Deposita, v. 39, p. 864–889.

Hemley, J.J., Montoya, J.W., Marinenko, J.W., and Luce, R.W., 1980, Equilibria in the system Al_2O_3-SiO_2-H_2O and some general implications for alteration-mineralization processes: Economic Geology, v. 75, p. 210–228.

Henley, R.W., and Berger, B.R., 2011, Magmatic-vapor expansion and the formation of high-sulfidation gold deposits: Chemical controls on alteration and mineralization: Ore Geology Reviews, v. 39, p. 63–74.

Henley, R.W., and McNabb, A., 1978, Magmatic vapor plumes and groundwater interaction in porphyry copper emplacement: Economic Geology, v.73, p. 1–20.

Herrington, R.J., Jankovic, S., and Kozelj, D., 1998, The Bor and Majdanpek copper-gold deposits in the context of the Bor metallogenic zone Serbia Yugoslavia, *in* Porter, T.M., ed., Porphyry and hydrothermal copper and gold deposits: A global perspective: Adelaide, GC Publishing, p. 185–194.

Hsu, L.C., 1986, The stability relationships of zunyite under hydrothermal conditions: Mining Geology, v. 36, p. 219–230.

Inan, E. E., and Einaudi, M. T., 2002, Nukundamite ($Cu_{3.38}Fe_{0.62}S_4$)–bearing copper ore at Bingham, Utah—Result of hydrothermal upflow through quartzite: Economic Geology, v. 97, p. 499–515.

Jannas, R.R., Beane, R.E., Ahler, B.A., and Brosnahan, D.R., 1990, Gold and copper mineralization at the El Indio deposit, Chile: Journal of Geochemical Exploration, v. 36, p. 233–266.

Knight, J., 1977, A thermochemical study of alunite, enargite, luzonite and tennantite deposits: Economic Geology, v. 72, p. 1321–1336.

Longo, A.A., 2000, The San Jose-Carachugo-Chaquicocha gold trend, Yanacocha district, northern Perú, *in* Cluer, J.G., Struhsacker, E.M., Hardyman, R.F., and Morris, C.L., eds., Geology and Ore Deposits 2000, The Great Basin and Beyond, Proceedings, v. 1, p. 201–220.

Longo, A.A., Dilles, J.H., Grunder, A.I., and Duncan, R., 2010, Evolution of calc-alkaline volcanism and associated hydrothermal gold deposits at Yanacocha, Peru: Economic Geology, v. 105, p. 1191–1241.

Maryono, A., Harrison, R.L., Cooke, D.R., Rompo, I., and Terence G. Hoschke, T.G., 2018, Tectonics and geology of porphyry Cu-Au Deposits along the Eastern Sunda magmatic arc, Indonesia: Economic Geology, v. 113, p. 7–38.

Meyer, C., and Hemley, J.J., 1967, Wall rock alteration, *in* Barnes, H.L., ed., Geochemistry of hydrothermal ore deposits: New York, Holt, Rhinehart and Winston, p. 166–232.

Muntean, J.L., and Einaudi, M.T., 2000, Porphyry gold deposits of the Refugio district, Maricunga belt, northern Chile: Economic Geology, v. 95, p. 1445–1472.

——2001, Porphyry-epithermal transition: Maricunga belt, northern Chile: Economic Geology, v. 96, p. 743–772.

Pilco, R., 2011, Hypogene alteration, sulfide mineralogy, and metal distribution at Cerro Yanacocha high-sulfidation epithermal deposit, northern Peru: Unpublished M.Sc. thesis, Tucson, University of Arizona, 89 p.

Pittuck, M., 2014, Technical Report NI43-101 on a mineral resource estimate on the Cukaru Peki deposit, Brestovac-Metovnica exploration permit, Serbia, January 28th 2014: Prepared for Reservoir Minerals Inc. by SRK Consulting, 82 p. (https://sedar.com/DisplayCompanyDocuments.do?lang=EN&issuerNo=00032332).

Pownall, J., and Lister, G., 2015, Seismotectonic analysis of Sumbawa region, 4D porphyry project: ANU Technical Report 2015-01, Confidential Report to sponsors, 8 p.

P.T. Sumbawa Timur Mining, 2020, Hu'u project, Onto copper-gold deposit, Nusa Tenggara Barat province, Indonesia, mineral resource estimate December 2019, 42 p. (http://sumbawatimurmining.co.id/mineral-resource-estimate-statement/).

Rainbow, A., Clark, A.H., Kyser, T.K., Gaboury, F., and Hodgson, C.J., 2005, The Pierina epithermal Au-Ag deposit, Ancash, Peru; paragenetic relationships, alunite textures, and stable isotope geochemistry: Chemical Geology, v. 215, p. 235–252.

Reyes, A.G., 1990, Petrology of Philippine geothermal systems and the application of alteration mineralogy to their assessment: Journal of Volcanology and Geothermal Research, v. 43, p. 279–309.

Ross, P-S., Hayman, P., and Núñez, G.C., 2017, Epithermal gold in felsic maar-diatremes: 14th SGA Biennial Meeting, Mineral Resources to Discover, 2017, v. 1, p. 331–334.
Sillitoe, R.H., 1983, Enargite-bearing massive sulfide deposits high in porphyry copper systems: Economic Geology, v. 78, p. 348–352.
——1994, Erosion and collapse of volcanoes: Causes of telescoping in intrusion-centered ore deposits: Geology, v. 22, p. 945–948.
——1999, Styles of high-sulphidation gold, silver and copper mineralization in porphyry and epithermal environments: Pacrim 1999, October 10–13,1999, Bali, Indonesia.
——2010, Porphyry copper systems: Economic Geology, v. 105, p. 3–41.
Stoffregen, R.E., 1987, Genesis of acid-sulfate alteration and Au-Cu-Ag mineralization at Summitville, Colorado: Economic Geology, v. 82, p. 1575–1591.
Teal, L., and Benavides, A., 2010, History and geologic overview of the Yanacocha Mining district, Cajamarca, Peru: Economic Geology, v. 105, p. 1173–1190.
Tessalina, S., 2015, Re-Os dating of molybdenite (Samples ID: 156908 and 156909) and pyrite (sample 156907): Vale Internal report, Report VALE_Moly, 5 p.
——2017, Report: Re-Os dating of two molybdenite samples (Samples ID: 622.2 and 590): Vale Internal report, Report_VALE_15112017, 3 p.
Vasconcelos, P., and Thiede, D., 2018, $^{40}Ar/^{39}Ar$ geochronology of alunite samples: UniQuest project no. C03292, Internal Vale report, 101 p.
Watanabe, Y., and Hedenquist, J.W., 2001, Mineralogic and stable isotope zonation at the surface over the El Salvador porphyry copper deposit, Chile: Economic Geology, v. 96, p. 1775–1797.
White, J.D.H., and Ross, P.S., 2011, Maar-diatreme volcanoes: A review: Journal of Volcanology and Geothermal Research, v. 201, p. 1–29.

David Burrows graduated in geology from Trinity College Dublin and then gained M.Sc. and Ph.D. degrees in economic geology from the University of Toronto, Canada. He is currently chief geologist for copper and nickel for the Vale Global Exploration and has over 30 years of experience in the mineral exploration in Vale since 2006, and before that with Inco. He has worked extensively in North and South America, Indonesia, Brazil, Australia, Europe, and Africa, in exploration programs for gold, porphyry copper, IOCG, VMS, and sediment-hosted copper and base metal deposits.